ESTIMATION OF DRAG ARISING FROM ASYMMETRY IN THRUST OR AIRFRAME CONFIGURATION

1. NOTATION AND UNITS*

		SI	*British*
A	wing aspect ratio, b^2/S		
A_F	effective aspect ratio of fin and rudder, $2h_F^2/S_F$		
b	wing span	m	ft
C_D	drag coefficient for aeroplane, D/qS		
C_{D_F}	drag coefficient for fin and rudder, D_F/qS_F		
$(C_{L_\alpha})_F$	lift-curve slope for straight-tapered wing of aspect ratio A_F, taper ratio, c_{t_F}/c_{r_F}, half-chord sweep angle $\Lambda_{½F}$, and area $2S_F$, estimated from Item No. 70011 (Reference 9), see Sections 6.1.1 and 6.1.2 here		
C_l	rolling moment coefficient for aeroplane, L/qSb		
C_n	yawing moment coefficient for aeroplane, N/qSb		
C_Y	sideforce coefficient for aeroplane, Y/qS		
C_{Y_F}	sideforce coefficient for fin and rudder, Y_F/qS_F		
c_r, c_t	wing root and tip chords	m	ft
c_{r_F}, c_{t_F}	fin root and tip chords	m	ft
D	drag of aeroplane	N	lbf
D_F	drag of fin and rudder	N	lbf
D_{wm}	windmilling drag, per engine	N	lbf
F_N	net thrust, per engine	N	lbf
g	acceleration due to gravity	m/s^2	ft/s^2
g_x; g_y; g_z	components of g in x-direction; y-direction; z-direction	m/s^2	ft/s^2
H	geopotential height	m	ft
h_B	fuselage maximum height	m	ft
h_F	fin height, measured from root chord, see Sketch 1.1, or height of equivalent single fin, see Equation (A2.9)	m	ft
J_B, J_T, J_W	sideforce correction factors defined in Reference 13		
K_F	induced drag factor for fin and rudder		
L	rolling moment	N m	lbf ft
L^Σ	resultant rolling moment	N m	lbf ft

* See also Section 1.1.

Issued December 1988
With Amendment A, September 1989

L_F	rolling moment due to fin and rudder	N m	lbf ft
L_v	rolling moment derivative due to sideslip*, $L_v = (\partial L/\partial v)/(\rho VSb/2) = \partial C_l/\partial\beta$		
L_ζ	rolling moment derivative due to rudder deflection*, $(\partial L/\partial\zeta)/qSb$	rad^{-1}	rad^{-1}
L_ξ	rolling moment derivative due to aileron deflection*, $(\partial L/\partial\xi)/qSb$	rad^{-1}	rad^{-1}
l_F	moment arm (from wing aerodynamic centre) of sideforce due to fin and rudder; used in method of Section 3, see Sketch 3.1	m	ft
l_p	moment arm of engine gross thrust or propeller thrust	m	ft
M	free-stream Mach number		
m	aeroplane mass	kg	slug
N	yawing moment	N m	lbf ft
N^Σ	resultant yawing moment	N m	lbf ft
N_F	yawing moment due to fin and rudder	N m	lbf ft
N_v	yawing moment derivative due to sideslip*, $N_v = (\partial N/\partial v)/(\rho VSb/2) = \partial C_n/\partial\beta$		
N_ζ	yawing moment derivative due to rudder deflection*, $(\partial N/\partial\zeta)/qSb$	rad^{-1}	rad^{-1}
N_ξ	yawing moment derivative due to aileron deflection*, $(\partial N/\partial\xi)/qSb$	rad^{-1}	rad^{-1}
p ; q ; r	angular velocity components about x-axis (rate of roll); y-axis (rate of pitch); z-axis (rate of yaw)	rad/s	rad/s
q	kinetic pressure, $\rho V^2/2$	N/m^2	lbf/ft^2
S	wing (reference) area	m^2	ft^2
S_F	fin and rudder area, see Sketch 1.1	m^2	ft^2
S_R	rudder area	m^2	ft^2
T	propeller thrust, per propeller	N	lbf
u ; v ; w	components of V in x-direction; y-direction; z-direction	m/s	ft/s
V	true airspeed (resultant velocity relative to air)	m/s	ft/s
x , y , z	aeroplane body-axis coordinates (origin at aeroplane centre of gravity), see Sketch 1.1	m	ft
x_F	moment arm (in yaw) for sideforce due to fin and rudder	m	ft
Y	sideforce, positive to starboard (in y-direction)	N	lbf
Y_F	sideforce due to fin and rudder	N	lbf
Y_v	sideforce derivative*, $Y_v = (\partial Y/\partial v)/(\rho VS/2) = \partial C_Y/\partial\beta$		
$(Y_v)_F$	fin contribution to Y_v		
Y_ζ	sideforce derivative due to rudder deflection*, $(\partial Y/\partial\zeta)/qS$	rad^{-1}	rad^{-1}
Y_ξ	sideforce derivative due to aileron deflection*, $(\partial Y/\partial\xi)/qS$	rad^{-1}	rad^{-1}
z_F	moment arm (in roll) for sideforce due to fin and rudder	m	ft

See footnote at end of Notation Section

β	angle of sideslip ($\sin\beta = v/V$)	deg	deg
ΔC_D	increment in aeroplane drag coefficient		
$(\Delta C_D)_F$	fin-and-rudder contribution to ΔC_D		
$\Delta C_{D_{asym\ thr}}$	increment in C_D due to thrust asymmetry		
$\Delta C_{D_{wm}}$	increment in C_D due to windmilling engine		
ΔC_L	change in wing lift coefficient needed to counteract rolling moment due to asymmetry, see Sections 6.4 and 6.5		
Δm	asymmetry in airframe mass	kg	slug
ζ	rudder deflection angle	rad	rad
η	spanwise coordinate, $y/(b/2)$		
Θ	inclination angle (elevation or angle of pitch) between horizontal and x-body-axis	deg	deg
$\Lambda_{¼F}$, $\Lambda_{½F}$	fin and rudder quarter-chord and half-chord sweep angles	deg	deg
ξ	aileron deflection angle	rad	rad
ρ	density of air	kg/m^3	slug/ft^3
Φ	bank angle, ($\Phi = 0$, wings level; $\Phi > 0$, starboard wing down)	deg	deg

Subscripts

aero	denotes airframe aerodynamic force or moment, except for those imposed by asymmetry and denoted by "asym"
aileron	denotes value for aileron
asym	denotes asymmetric force or moment imposed on aircraft
feathered	denotes value with feathered propeller
ind	denotes induced drag component
n	denotes *n*'th fin in multiple-fin configuration
profile	denotes profile drag component
sideslip	denotes value for flight in sideslip for aircraft minus fin
$\beta = 0$	denotes flight condition with zero sideslip
$\zeta = 0$	denotes flight condition with zero rudder deflection
$\Phi = 0$	denotes flight condition with wings level

* See Section 1.1.

1.1 Use of Control and Stability Derivative Data

This Item follows the definitions and nomenclature used in the ESDU Aerodynamics Series for control and stability derivatives. The derivatives L_v, *etc.* are formally defined for a datum condition of steady, rectilinear flight at zero sideslip. The equivalence to coefficient derivatives, $\partial C_l/\partial\beta$, *etc.*, holds for these conditions, see Reference 33. The subscript "*e*", used to denote datum conditions in the Aerodynamics Series, is omitted here. Conversions to forms customarily used in the USA are as follows.

Derivative used here	L_v	L_ζ	L_ξ	N_v	N_ζ	N_ξ	Y_v	Y_ζ	Y_ξ
USA equivalent	C_{l_β}	$C_{l_{\delta R}}$	$C_{l_{\delta A}}$	C_{n_β}	$C_{n_{\delta R}}$	$C_{n_{\delta A}}$	C_{Y_β}	$C_{Y_{\delta R}}$	$C_{Y_{\delta A}}$

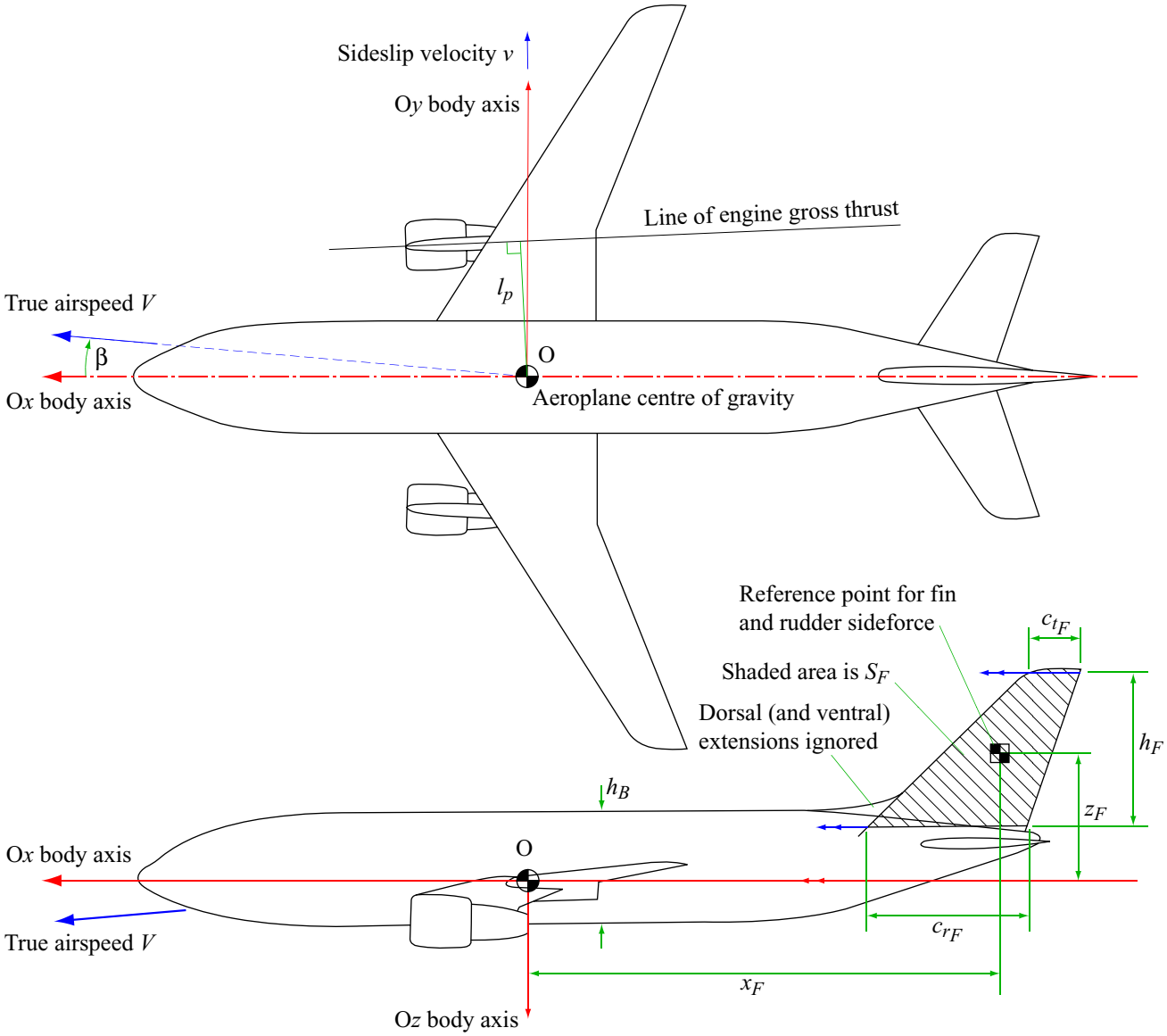

Sketch 1.1 Axes, dimensions and angles

2. INTRODUCTION

Methods are provided for estimating drag increments arising in steady trimmed flight as a consequence of asymmetry in thrust or airframe configuration. The primary application is to flight with one or more engines inoperative as, for example, in calculations of climb performance after take-off or a missed approach where the drag due to asymmetry can be greater than the drag due to the inoperative engine at low speeds, see Sketch 2.1. Thrust asymmetry may also be significant in range calculations if a long diversion becomes necessary because of engine failure.

The Data Item can, however, be used to consider asymmetries in thrust, drag, lift and mass since these are counteracted in related ways. The significant factors are the relative magnitudes of the yawing and rolling moments imposed on the aircraft and the piloting techniques used, that is, the combination of control inputs applied about the yaw and roll axes.

Section 3 provides a simple method, based on established data for a wide range of aeroplanes, for predicting the drag increment for flight with one or more engines inoperative (excluding the drag of the inoperative engine). The broad effects on drag of different flight techniques are shown but, because of a lack of detailed information for individual aeroplanes, no information is given on the breakdown of drag into components. The correlating parameter used is derived in Appendix A.

Section 4 gives the force and moment equations used to determine equilibrium flight conditions for use with aerodynamic data. Results of such calculations are shown in sketch form while a detailed example is given as Appendix B.

Section 5 provides a detailed discussion of the alternative ways in which an aircraft can be flown to achieve steady straight flight in the presence of thrust or airframe asymmetries. Practical aspects of obtaining and using flight-test and wind-tunnel data are discussed.

Section 6 lists the various drag components that can arise as a consequence of thrust and airframe asymmetries and gives methods for estimating some of them. Where the estimation procedure involves the use of Data Items from the ESDU Aerodynamics Series, typical values of the drag components are presented.

Appendix A derives the relationships between asymmetric forces tending to yaw the aircraft and the fin/rudder side force and induced drag corresponding to equilibrium flight.

Appendix B presents an example of the use of wind-tunnel data, in conjunction with the equations for equilibrium flight conditions from Section 4, to estimate the drag due to asymmetry in thrust.

2.1 Relationship Between Lateral/Directional Trim and Longitudinal Trim

The methods given are concerned primarily with the effects, on drag, of establishing the lateral/directional trim of the aeroplane in the presence of thrust or airframe asymmetries, However, it is likely that changes in longitudinal trim will occur between corresponding symmetric and asymmetric flight conditions, for example, the loss of thrust of an engine may introduce a large change in pitching moment.

In all Sections except Section 3 it is assumed that forces along and moments about all three aircraft axes can be considered independently, *i.e.* that there is no cross coupling between lateral/directional and longitudinal trim changes, and no further consideration is given to longitudinal trim. Note that for some aeroplane configurations there may be significant interactions between lateral/directional and longitudinal trim changes, for example if wing downwash is affected by changes in directional and/or lateral control or in power settings.

In Section 3 and Figures 1, 2 and 3 the increment in drag coefficient due to asymmetry in thrust includes all drag components except the windmilling drag of the inoperative engine or propeller.

2.2 Methods For Estimating Drag of Inoperative Powerplants

The Performance Series includes methods of estimating windmilling drag of propellers (Item No. ED1/1, Reference 1), windmilling drag of jet and fan engines (Item No. 81009, Reference 2) and spillage drag of axisymmetric intakes (Item No. 84004, Reference 3). The combined usage of References 2 and 3 is demonstrated in Reference 4.

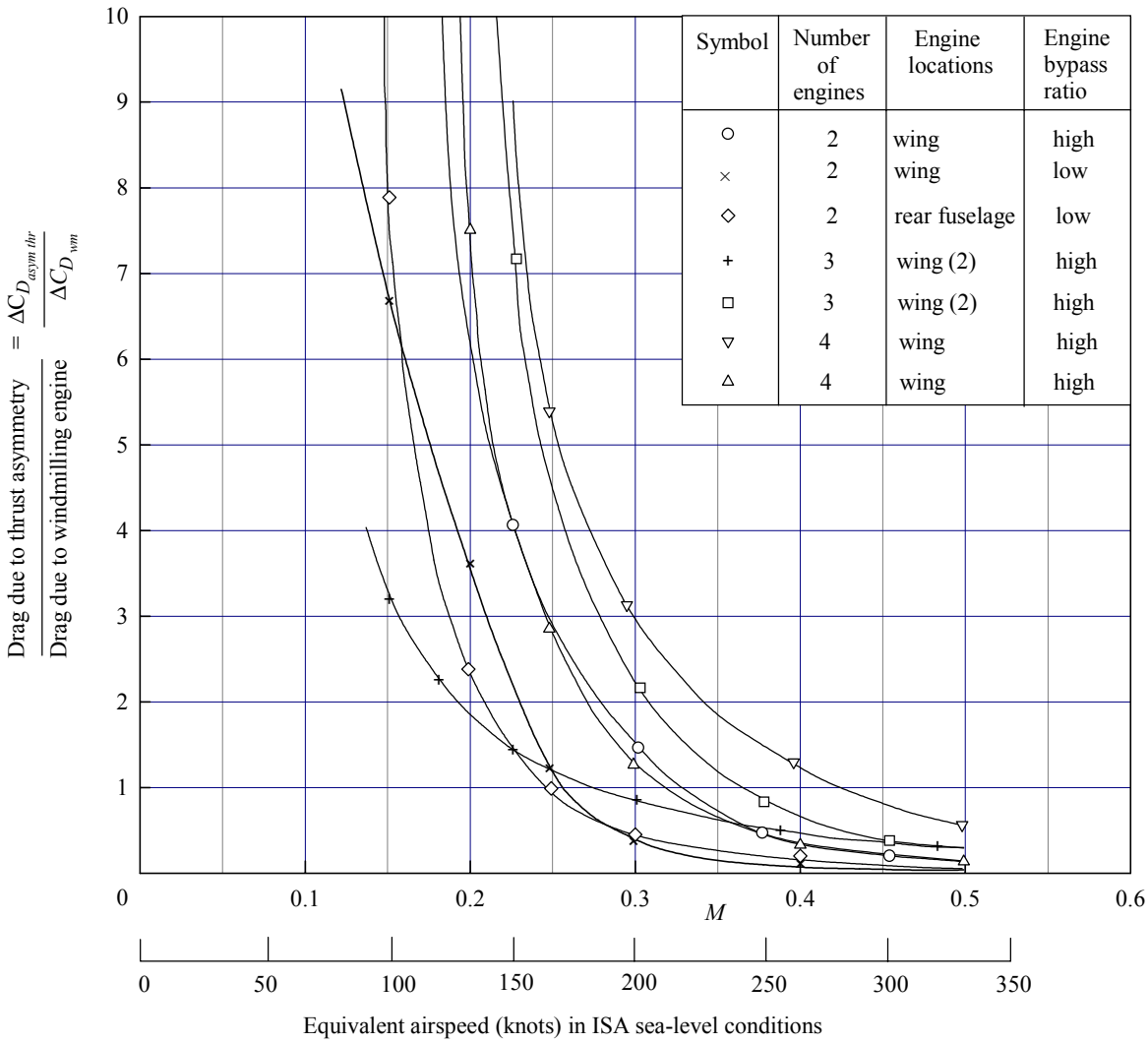

Sketch 2.1 Examples of relative magnitudes of drag due to thrust asymmetry and engine windmilling drag

3. FIRST APPROXIMATION TO AIRFRAME DRAG COEFFICIENT INCREMENT FOR STEADY STRAIGHT FLIGHT WITH FAILED ENGINE(S)

Figures 1, 2 and 3 present data for use in estimating values of $\Delta C_{D_{asym\ thr}}$, the increment in airframe drag coefficient due to thrust asymmetry.

3.1 Method of Estimating $\Delta C_{D_{asym\ thr}}$

Values of $\Delta C_{D_{asym\ thr}}$ are presented in Figures 1, 2, 3 as functions of the parameter

$$\frac{1}{2\pi}\left(\frac{N_{asym}}{q}\right)^2\left(\frac{1}{l_F h_F}\right)^2\frac{1}{S}.$$

The imposed yawing moment, N_{asym}, for a symmetrically located pair of powerplants, is

$$N_{asym} = (\text{thrust difference between powerplants})\ l_p,$$

where the moment arm, l_p is defined in Sketch 1.1. Where one of the pair of powerplants is inoperative,

$$N_{asym} = (F_N + D_{wm})l_p \text{ for jet and fan engines,}$$
$$N_{asym} = (T + D_{feathered})l_p \text{ or } (T + D_{wm})l_p \text{ for propellers.}$$

The wing (reference) area, S, used in the correlating parameter and in defining $\Delta C_{D_{asym\ thr}}$ is the equivalent straight-tapered gross wing defined in Sketch 3.1. Values of the fin and rudder moment arm, l_f, should be determined as indicated in Sketch 3.1.

For a single vertical fin the height h_F and area S_F are as shown in Sketch 1.1. For multiple-fin configurations,

$$\frac{1}{h_F^2} = \frac{\Sigma\left(\frac{S_{F_n}}{h_{F_n}}\right)^2}{(\Sigma S_{F_n})^2}.$$

See Section A2.3 of Appendix A for the derivation of this expression and for advice regarding the selection of appropriate values of h_{F_n} and S_{F_n}. For non-vertical fins, h_{F_n} and S_{F_n} are taken as the projected values in the aeroplane plane of symmetry.

3.2 Estimation of $\Delta C_{D_{asym\ thr}}$ for Different Flight Techniques* and Airframe/Powerplant Combinations

For jet- and fan-engined aeroplanes (Figures 1 and 2) it should be assumed that the only drag component excluded from $\Delta C_{D_{asym\ thr}}$ is the engine windmilling (*i.e.* internal) drag, D_{wm}, and that cowl spillage drag is included in Figures 1 and 2 (see Reference 2 for method of estimating windmilling drag).

For propeller-driven aeroplanes (Figures 2 and 3) it should be assumed that the only drag component excluded is that of the feathered or (less likely) windmilling propeller (see Reference 1 for method of estimating windmilling drag).

* See Section 5.1 and Sketches 5.1 to 5.4 regarding the various flight techniques.

For flight with "roll controls centralised*", for jet- and fan-engined aeroplanes, Figure 1 provides data for estimating values of $\Delta C_{D_{asym\ thr}}$ based on established data for 25 aeroplanes.

For flight with "significant sideslip, including wings level*", Figure 2 provides data for estimating values of $\Delta C_{D_{asym\ thr}}$ for both propeller-driven and jet- and fan-engined aeroplanes. The data for the 7 jet- and fan-engined aeroplanes used were for wings level. Of the 18 propeller-driven aeroplanes for which data are included in Figure 2, three were for wings level. The only data for propeller-driven aeroplanes excluded from Figure 2 were those ("for zero sideslip*") used in Figure 3. The use in Figure 2 of the parameter $(h_F/h_B)^2$ implies that much of the drag is induced by the aircraft body in sideslip.

For flight with "zero sideslip*", for propeller-driven aeroplanes, Figure 3 gives a rough guide, based on data for 4 aeroplanes.

For flight with "zero sideslip*", for jet- and fan-engined aeroplanes, the fin and rudder induced drag is the major component and a guide to its magnitude is given in Figures 1 and 2. More detailed estimates may be made using the methods of Section 6.1.2 and 6.2 for fin and rudder induced drag and profile drag, respectively.

For flight with zero rudder deflection*, for jet- and fan-engined aeroplanes, limited data (for 2 very different configurations) suggest, as might be expected, that values of $\Delta C_{D_{asym\ thr}}$ lie between those obtained from Figure 1 for roll controls centralised* and those from Figure 2 for flight with significant sideslip, including wings level.

3.3 Basis of Figures 1, 2 and 3

The data used to generate curves in Figures 1, 2 and 3 are either determined from, or confirmed by, flight tests and have been used in generating flight-manual data for the aircraft concerned. The primary correlating parameter is derived in Appendix A. Its use implies the following assumptions.

(i) The yawing moment due to asymmetric engine or propeller thrust is balanced by the moment due to fin and rudder sideforce.

(ii) The drag due to asymmetry is made up entirely of the induced drag corresponding to the fin and rudder sideforce.

Assumption (i) is reasonable for flight with zero sideslip* but for straight flight this implies that the aircraft must be banked. In practice, some combination of bank and sideslip is likely but for most of the aircraft for which data were available these angles were unknown. In general, bank angles are of order 2 to 4 degrees and for civil transport aeroplanes some airworthiness requirements stipulate a maximum bank angle of 5 degrees. In practice, it may be preferred to fly with roll controls centralised (to avoid actuation of spoilers and/or to enhance the repeatability of flight-test results) or with wings level (to simplify piloting technique – particularly in instrument flight conditions).

Given that a combination of bank and sideslip angles is likely, the list of possible components of drag given in Section 6 indicates that while the fin and rudder induced drag may be the dominant term for flight with zero sideslip, this is unlikely to be true for other flight conditions. The extent to which assumption (ii) is invalid can be gauged from Figures 1, 2 and 3 by noting the departure of the aircraft data from the region labelled "fin and rudder induced drag".

* See Section 5.1 and Sketches 5.1 to 5.4 regarding the various flight techniques.

Difficulties associated with obtaining consistent measurements of drag due to asymmetry are discussed in Section 5. These are accentuated if no system of thrust and drag accounting is specified in the sources of data used. In particular, when analysing data for some aeroplanes it was not clear whether cowl spillage drag (if present) was included in "engine windmilling drag" or in the drag due to asymmetry. The analyses of data supporting Figures 1 to 3 (and other aspects of the Data Item) are reported in Reference 35.

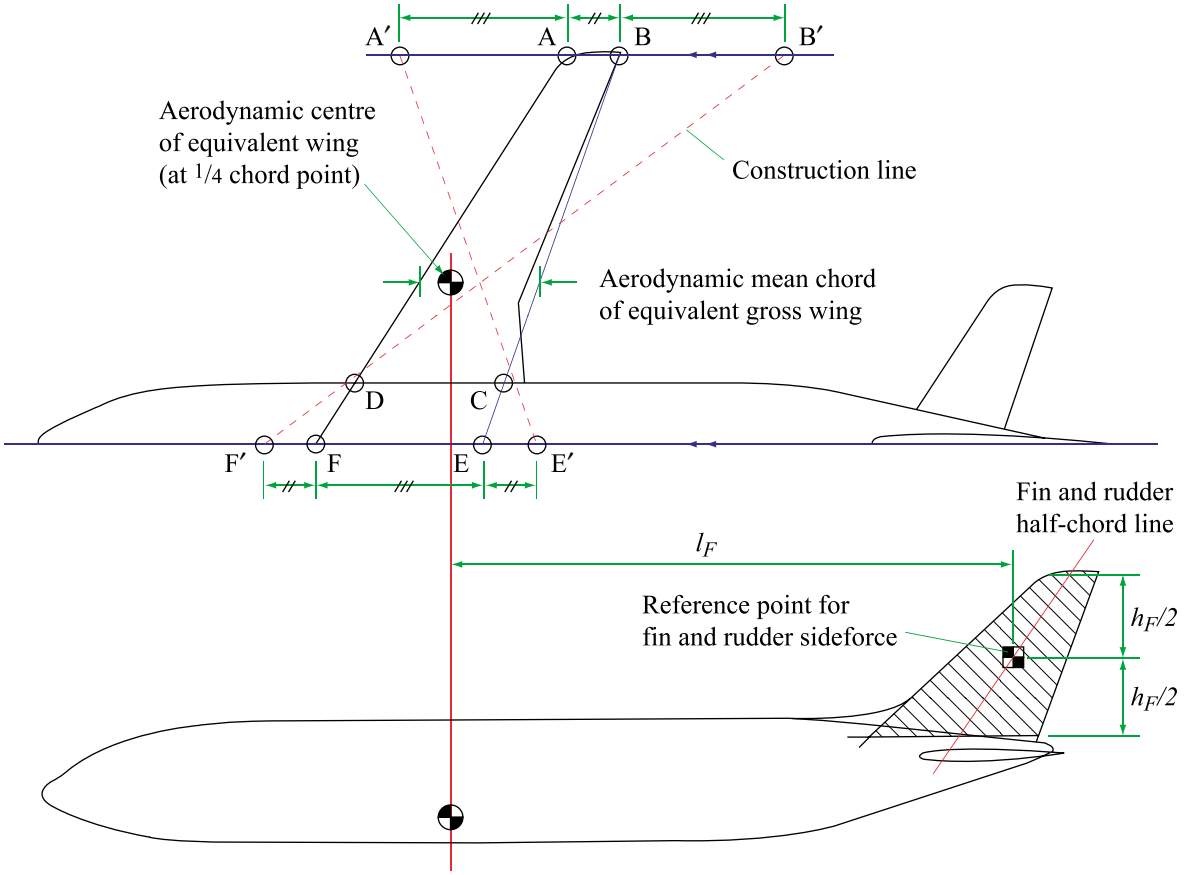

Procedure

(i) Construct equivalent straight-tapered wing ABCD having same exposed area as actual wing.
(ii) Extend AD to F and BC to E on centre line to give equivalent straight-tapered gross wing ABEF.
(iii) Identify A′, B′ at distances EF from A and B. Identify E′, F′ at distances AB from E and F.
(iv) Locate mean chord of equivalent gross wing at intersection of A′E′ and B′F′.
(v) Aerodynamic centre is located at 1/4 chord point.

Sketch 3.1 Approximate method used to estimate fin and rudder moment arm l_F

(Section 3 and Figures 1 and 2 only)

4. ESTIMATION OF EQUILIBRIUM FLIGHT CONDITIONS AND ASSOCIATED DRAG

Systematic methods of estimating the drag due to asymmetry utilise aerodynamic data for sideforce and for yawing and rolling moments to determine sideslip angles, bank angles and control deflections for steady straight flight and, then, evaluate the corresponding airframe drag increments. Equations for establishing the equilibrium flight conditions are presented in Section 4.1 while Section 4.2 discusses methods of solution and presents some simplifications for particular flight cases.

Where wind-tunnel data are used as the basis of estimation, the resulting increment in airframe drag coefficient (for a given configuration and values of angle of attack and Mach and Reynolds numbers) is

$$\Delta C_D = f(\beta, \zeta, \xi). \tag{4.1}$$

Appendix B presents an example based on wind-tunnel data.

Where estimated aerodynamic data are used, individual contributions to drag are likely to be evaluated separately. If the contributions to drag are those considered in Section 6 then, for example,

$$\Delta C_D = (\Delta C_D)_F + \Delta C_{D_{sideslip}} + \Delta C_{D_{aileron}} + \Delta C_{D_{spoiler}} + \Delta C_{D_{slipstream}}. \tag{4.2}$$

Other subdivisions of drag due to asymmetry are possible. Sketch 4.1 shows an example of the variation, with sideslip angle, of estimated values of contributions to drag due to asymmetric thrust for a large transport aeroplane in the take-off configuration (Reference 31). The sketch illustrates an alternative subdivision of the terms $[(\Delta C_D)_F + \Delta C_{D_{sideslip}}]$ in that the broken line which passes through the origin represents the "drag due to sideslip" of the whole aircraft at zero rudder deflection, to which a "rudder drag" contribution is added.

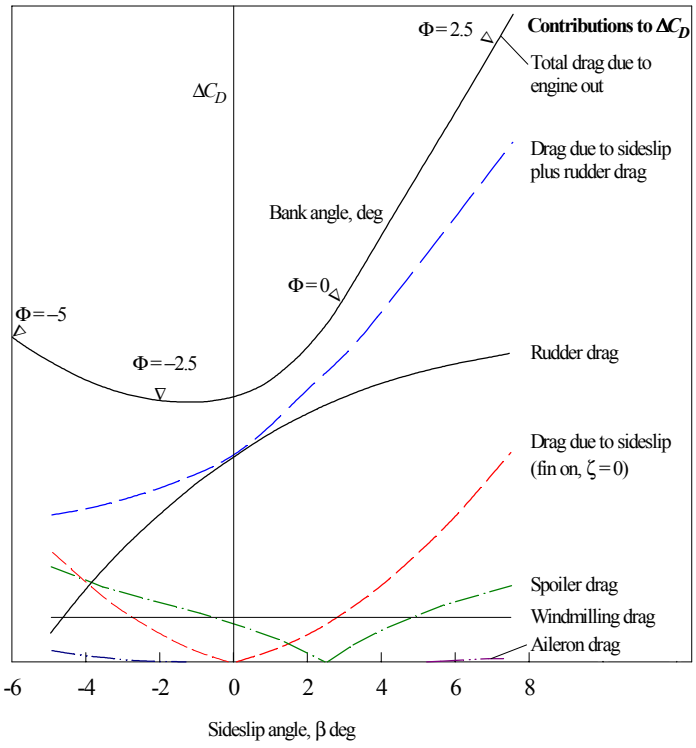

Sketch 4.1 Example of drag coefficient increments resulting from balancing lateral-directional asymmetry due to failed engine in take-off climb configuration

4.1 Equations for Equilibrium Flight Conditions

For trimmed, steady straight flight the resultant sideforce, rolling moment and yawing moment acting on the aeroplane must be zero. These conditions may be expressed in terms of forces along the *y*-body axis and moments about the *x*- and *z*-body axes, as follows.

$$Y^{\Sigma} = Y_{aero} + mg\sin\Phi\cos\Theta + Y_{asym} = 0, \tag{4.3}$$

$$L^{\Sigma} = L_{aero} + L_{asym} = 0, \tag{4.4}$$

$$N^{\Sigma} = N_{aero} + N_{asym} = 0. \tag{4.5}$$

If wind-tunnel data are used as the basis for solving Equations (4.3) to (4.5), these data may be expressed in the form of sideforce, rolling and yawing moment coefficients* C_Y, C_l, C_n. For a given airframe configuration, and fixed values of angle of attack and Mach and Reynolds numbers, these coefficients are functions of β, ζ, ξ. The corresponding terms in Equations (4.3) to (4.5) are

$$Y_{aero} = qSC_Y, \tag{4.6}$$

$$L_{aero} = qSbC_l, \tag{4.7}$$

$$N_{aero} = qSbC_n. \tag{4.8}$$

Where estimated aerodynamic data are used as the basis for solving Equations (4.3) to (4.5), one method of expanding the equations to represent the various force and moment components is as follows:

$$Y^{\Sigma} = Y_F + Y_{sideslip} + Y_{aileron} + mg\sin\Phi\cos\Theta + Y_{asym} = 0, \tag{4.9}$$

$$L^{\Sigma} = L_F + L_{sideslip} + L_{aileron} + L_{asym} = 0, \tag{4.10}$$

$$N^{\Sigma} = N_F + N_{sideslip} + N_{aileron} + N_{asym} = 0. \tag{4.11}$$

If control and stability derivative data are to be used to obtain solutions to Equations (4.3) to (4.5) (as in Appendix B), these equations must be expressed in terms of the notation used in the Aerodynamics Series for stability derivatives to give

$$(Y_v \times v)\frac{\rho VS}{2} + (Y_\zeta \times \zeta)qS + (Y_\xi \times \xi)qS + mg\sin\Phi\cos\Theta + Y_{asym} = 0, \tag{4.12}$$

$$(L_v \times v)\frac{\rho VS\,b}{2} + (L_\zeta \times \zeta)qSb + (L_\xi \times \xi)qSb + L_{asym} = 0, \tag{4.13}$$

$$(N_v \times v)\frac{\rho VS\,b}{2} + (N_\zeta \times \zeta)qSb + (N_\xi \times \xi)qSb + N_{asym} = 0. \tag{4.14}$$

Further alternative forms of these equations can be written if force or moment data are likely to be available in coefficient form, for example, for the yawing moment due to sideslip the term,

$$(N_v \times v)\frac{\rho VS\,b}{2} = \left(\frac{\partial N}{\partial v} \times v\right)\frac{\rho VS\,b}{2} = \left(\frac{\partial C_n}{\partial \beta} \times \beta\right)qSb. \tag{4.15}$$

In such cases, however, it is more likely that the approach of Equations (4.3) to (4.8) will be used.

* As quoted, the coefficients C_Y, C_l, C_n accord with those used in the ESDU Aerodynamics Series. Other methods of rendering these quantities non-dimensional are in use, for example wing chord may be used in place of span, *b*.

4.2 Solution of Equations for Equilibrium Flight Conditions

Equations (4.3) to (4.5), (4.9) to (4.11) or (4.12) to (4.14) must be solved to determine the values of sideslip and bank angles and rudder and aileron (or spoiler) deflections that correspond to trimmed steady straight flight. However, various simplifying assumptions can be made regarding the representation of the imposed asymmetric force and moments and the solution of the equations for particular cases. These are considered in Sections 4.2.1 and 4.2.2 respectively.

4.2.1 Representation of imposed asymmetric force and moment

In Section 4.1 the terms representing the imposed asymmetric sideforce and moments in Equations (4.3) to (4.5), (4.9) to (4.11) and (4.12) to (4.14) allow all forms of asymmetry to be considered, for example, asymmetries in thrust, drag, lift and mass.

For asymmetry in thrust, the full expressions for body-axis components of forces and moments due to engine gross thrust, momentum drag, propeller thrust and propeller in-plane force are given in Tables 6.3 and 6.4 of Item No. 85030 (Reference 8). In practice, many of the terms involved (particularly those involving more than one small angle) can be ignored.

The simplest expression for N_{asym}, for a symmetrically located pair of powerplants, is

$$N_{asym} = (\text{thrust difference between powerplants})\ l_p,$$

so that where one of a symmetric pair of powerplants is inoperative,

$$N_{asym} = (F_N + D_{wm})l_p \text{ for jet and fan engines,} \tag{4.16}$$

$$N_{asym} = (T + D_{feathered})l_p \text{ or } (T + D_{wm})l_p \text{ for propellers.} \tag{4.17}$$

Equations (4.16) and (4.17) take no account of different lines of action of the forces but, if differences exist, the moment arm, l_p, should be selected to take account of any "toe-in" or "toe-out" of the engine gross thrust or propeller thrust vectors. The term representing the drag of the inoperative powerplant (D_{wm} or $D_{feathered}$ here) should strictly include all drag changes due to the inoperative engine, *i.e.* in spillage drag, and in slipstream drag behind a propeller or jet or fan engine ("scrubbing drag"). However for the purposes of calculating N_{asym} (but not for drag calculations) it is permissible to omit many of the smaller terms, such as the drag of a feathered propeller.

For asymmetry in airframe lift and/or drag, Item No. 85030 (Reference 8) gives definitions of both the air-path-axis (Table 6.5) and body-axis (Table 6.6) components of airframe and control aerodynamic forces and moments. Note that Equations given in Section 4.1 here are expressed in terms of body-axis components of forces and moments but that the customary methods of presenting aerodynamic data* provide values of rolling and yawing moment coefficients about the "aerodynamic-body axes" (or "wind axes" or "stability axes"). For small angles of attack and sideslip the differences can be overlooked but, if large angles are likely, the appropriate body-axis components should be derived (see Table 6.2 of Reference 8 for axis-transformation formulae).

* Most wind-tunnel data are presented in terms of these axes and the practice is adhered to in the ESDU Aerodynamics Series.

For asymmetry in airframe mass of magnitude Δm, located at point (x, y, z) relative to the position (in the absence of Δm) of the aeroplane centre of gravity, the expressions for Y_{asym}, L_{asym} and N_{asym} are

$$Y_{asym} = \Delta m g_y = \Delta m g \sin\Phi \cos\Theta, \quad (4.18)$$

$$L_{asym} = \Delta m(y g_z - z g_y) = \Delta m g(y \cos\Phi \cos\Theta - z \sin\Phi \cos\Theta), \quad (4.19)$$

$$N_{asym} = \Delta m(-y g_x + x g_y) = \Delta m g(y \sin\Theta + x \sin\Phi \cos\Theta). \quad (4.20)$$

4.2.2 Simplifications to equations for equilibrium flight conditions

From the discussions presented in Section 5, a number of simplifying assumptions can be made for particular flight cases. Although the remarks made here apply regardless of whether wind-tunnel or estimated aerodynamic data are used, they are illustrated by reference to Equations (4.12) to (4.14).

(i) **For flight with wings level,** $\Phi = 0$ so the term involving Φ in Equation (4.12) vanishes; but aileron and/or spoiler deflections depend on the size of any rolling moment to be counteracted.

(ii) **For flight with zero sideslip,** $v = \beta = 0$ so that the first term in each of Equations (4.12) to (4.14) vanishes but bank angle $\Phi \neq 0$.

(iii) **For flight with roll controls centralised,** the aileron and/or spoiler deflections are zero or very small so that terms involving ξ may be ignored.

(iv) **For flight with rudder centralised,** terms involving ζ become zero.

(v) **For some calculation purposes** the following terms, which for some configurations represent adverse secondary effects of control deflections, may be neglected as of second order compared to the others.

rolling moment due to rudder, *i.e.* L_ζ term in Equation (4.13)
yawing moment due to aileron, *i.e.* N_ξ term in Equation (4.14).

(vi) **For nearly all calculations** it is possible to neglect the sideforce due to aileron deflection *i.e.* Y_ξ term in Equation (4.12).

(vii) **For flight with wings level with an asymmetric yawing moment,** and where simplifications (v) and (vi) apply, Equations (4.12) and (4.14) become.

$$(Y_v \times v)\frac{\rho V S}{2} + (Y_\zeta \times \zeta) q S = 0, \quad (4.21)$$

$$(N_v \times v)\frac{\rho V S b}{2} + (N_\zeta \times \zeta) q S b = -N_{asym}. \quad (4.22)$$

By substituting $v = V \sin\beta$ in Equations (4.21) and (4.22) they can be expressed in the forms

$$(Y_v \times \sin\beta) + (Y_\zeta \times \zeta) = 0, \quad (4.23)$$

$$(N_v \times \sin\beta) + (N_\zeta \times \zeta) = \frac{-N_{asym}}{q S b} \quad (4.24)$$

from which

$$\sin\beta_{\Phi = 0} = \frac{-N_{asym}}{q S b\left[N_v - N_\zeta \frac{Y_v}{Y_\zeta}\right]}. \quad (4.25)$$

(viii) **For flight with zero sideslip with an asymmetric yawing moment,** and where simplifications (v) and (vi) apply, Equations (4.12) and (4.14) become

$$(Y_\zeta \times \zeta)\frac{qS}{2} + mg\cos\Theta\sin\Phi_{\beta=0} = 0, \tag{4.26}$$

$$(N_\zeta \times \zeta)\frac{qSb}{2} = -N_{asym} \tag{4.27}$$

from which

$$\Phi_{\beta=0} = \sin^{-1}\left[\frac{-(Y_\zeta \times \zeta)}{mg\cos\Theta} \times \frac{qs}{2}\right] \approx \sin^{-1}\left[\frac{-(Y_\zeta \times \zeta)}{C_L}\right], \tag{4.28}$$

$$\zeta_{\beta=0} = \frac{-N_{asym}}{N_\zeta \times qSb} \tag{4.29}$$

or, by combining Equations (4.28) and (4.29),

$$\Phi_{\beta=0} = \sin^{-1}\left[\frac{N_{asym}}{b}\frac{Y_\zeta}{mg\cos\Theta N_\zeta}\right]. \tag{4.30}$$

Note that the use of different methods of rendering aerodynamic parameters non-dimensional, may result in, for example, wing chord replacing span, b, in Equations (4.24), (4.25), (4.27), (4.29) and (4.30).

4.2.3 General solutions for case with asymmetric yawing moment

Equations (4.12) and (4.14) are used here to derive general relationships for the case of an aeroplane in trimmed flight with an asymmetric yawing moment but ignoring the effects of aileron and/or spoiler deflections. From Equation (4.14), if the substitution $v = V\sin\beta$ is made, the rudder angle to trim can be expressed as

$$\zeta = -\frac{1}{N_\zeta}\left[\frac{N_{asym}}{qSb} + N_v\sin\beta\right]. \tag{4.31}$$

If the same substitution is made in Equation (4.12), that Equation may be solved simultaneously with Equation (4.31) to give

$$\sin\beta = \frac{1}{qS}\frac{\left[\frac{Y_\zeta}{N_\zeta}\frac{N_{asym}}{b} - (mg\sin\Phi\cos\Theta)\right]}{\left[Y_v - \frac{Y_\zeta}{N_\zeta}N_v\right]} \tag{4.32}$$

and

$$\zeta = \frac{1}{qS}\frac{\left[\frac{Y_v}{N_v}\frac{N_{asym}}{b} - (mg\sin\Phi\cos\Theta)\right]}{\left[Y_\zeta - \frac{Y_v}{N_v}N_\zeta\right]}. \tag{4.33}$$

By using the relationships developed in Equations (4.25) and (4.30), it can be shown that for this case the bank and sideslip angles to trim are related by

$$\frac{\sin\beta}{\sin\beta_{\Phi=0}} = 1 - \frac{\sin\Phi}{\sin\Phi_{\beta=0}}. \tag{4.34}$$

Similarly, it can be shown that the bank and rudder angles to trim are related by

$$\frac{\zeta}{\zeta_{\Phi=0}} = 1 - \frac{\sin\Phi}{\sin\Phi_{\zeta=0}}. \tag{4.35}$$

Combining Equations (4.34) and (4.35) leads to the following general relationship for bank, sideslip and rudder angles to trim,

$$\frac{\sin\beta}{\sin\beta_{\Phi=0}} = 1 + \left[\frac{\zeta}{\zeta_{\Phi=0}} - 1\right]\frac{\sin\Phi_{\zeta=0}}{\sin\Phi_{\beta=0}}. \tag{4.36}$$

The effects of aileron and/or spoiler deflections can of course be included in these results if the appropriate terms (*i.e.* those involving ξ) are not deleted from Equations (4.12) and (4.14). Alternatively, the particular flight condition corresponding to $\xi = 0$ can be deduced by noting that for this condition Equation (4.13) reduces to

$$L_v \sin\beta + L_\zeta \zeta = 0. \tag{4.37}$$

5. PRACTICAL CONSIDERATIONS

Sketch 5.1
Flight with asymmetric thrust and zero bank

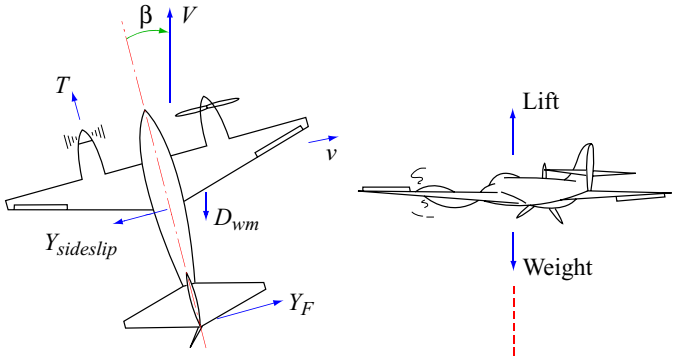

Sketch 5.2
Flight with asymmetric thrust and zero sideslip

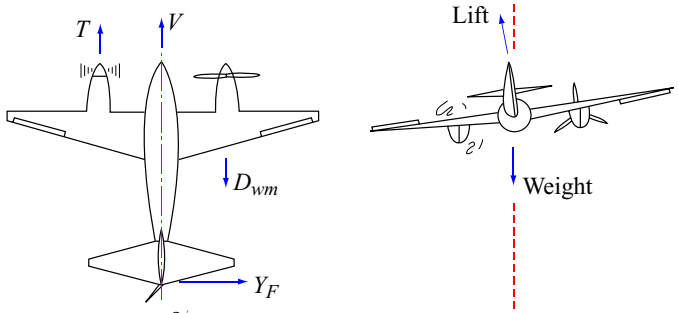

Sketch 5.3
Flight with asymmetric thrust and sideslip towards live engine

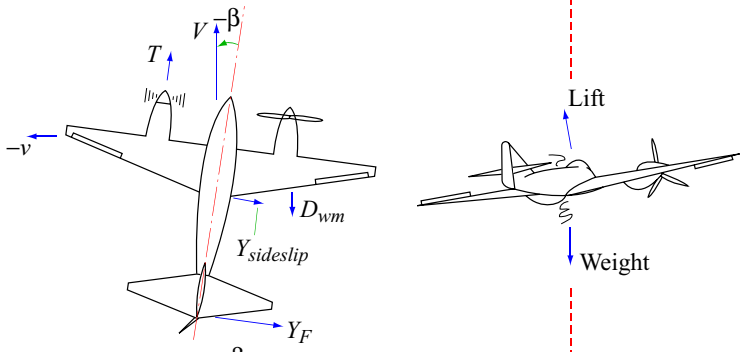

Sketch 5.4
Flight with asymmetric thrust and rudder central

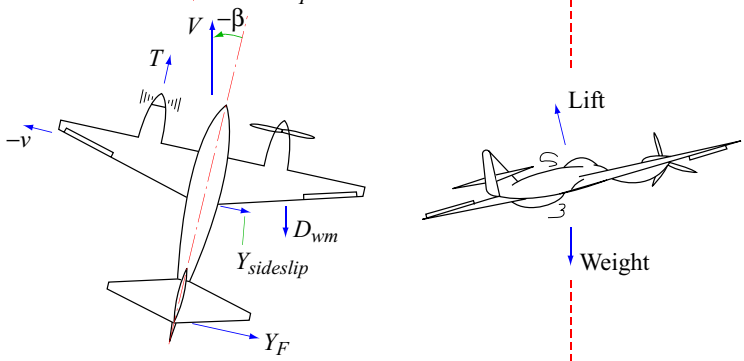

Sketch 5.5
Flight with asymmetric thrust and dead-engine down

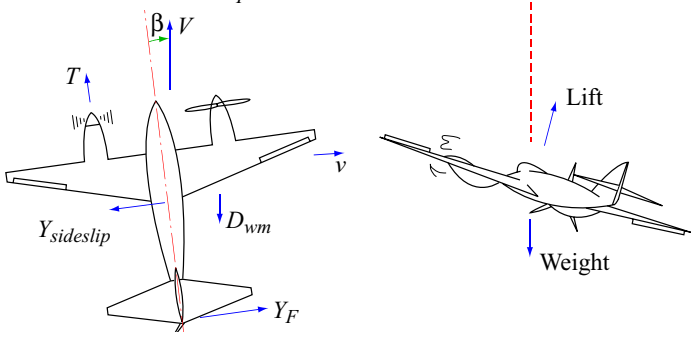

5.1 Conditions for Steady Straight Flight with Asymmetric Engine or Propeller Thrust

There are an infinite number of combinations of bank and sideslip angles and of rudder and aileron and/or spoiler angles under which steady straight asymmetric flight can be achieved. Seven categories of flight condition are identified and discussed in paragraphs (a) to (g) and most of these are illustrated in Sketches 5.1 to 5.5 (views from vertically above and along the air-path vector, V,). For simplicity, the sketches show only the major powerplant and airframe-aerodynamic forces (and weight) although for trimmed, steady, straight flight each of the following conditions must be met (see Section 4.1).

(i) Resultant sideforce is zero, so that there is no acceleration perpendicular to the direction of motion (the necessary condition for straight flight).
(ii) Resultant yawing moment is zero (the necessary condition for the aeroplane to maintain constant heading and thus constant angle of sideslip).
(iii) Resultant rolling moment is zero (the necessary condition for the aeroplane to maintain a constant bank angle).

(a) Flight with wings level. In this condition the relevant forces on the aeroplane are as shown in Sketch 5.1. The aeroplane is sideslipping towards the dead engine with the rudder to the opposite side. The rudder and angle of sideslip have been adjusted by the pilot until there is no resultant side force on the aircraft, and also no resultant yawing moment. Ailerons (and/or spoilers) are used as necessary to maintain wings-level flight. This flight condition is relatively simple to establish (in both visual and instrument flight conditions) but the associated drag penalty may be severe.

(b) Flight with roll controls centralised, *i.e.* zero aileron and spoiler deflections. As in (a), above, rudder is used to counter the asymmetric yawing moment and the aeroplane sideslips towards the dead engine. Since ailerons or spoilers are not used, the rolling moment due to fin and rudder sideforce must be countered by the rolling moment due to sideslip (L_v) of the rest of the airframe. For jet- and fan- engined aeroplanes a state of equilibrium is usually reached at quite small angles of bank. For such aeroplanes the technique is advantageous because of the avoidance of aileron and, more particularly, spoiler drag and the relative ease with which test results may be repeated. The technique is applied in the certification of many jet- and fan-engined transport aeroplanes but is unlikely to be acceptable for propeller-driven aeroplanes because of the larger bank angles likely due to the lift loss associated with the failed engine.

(c) Flight with zero sideslip. The forces acting now are shown in Sketch 5.2. The aeroplane is banked with the live engine wing down and rudder applied to the same side to counteract the yawing moment due to asymmetric thrust. The side component of the wing lift balances the sideforce on the fin and rudder due to the rudder deflection. The angle of bank required to reduce the sideslip to zero is normally only two or three degrees and the rudder angle is less than that required in case (a) above. The pilot will find it impossible to maintain this flight condition unless he has a special sideslip indicator or some other indication (such as a head-up display with appropriate air-data inputs, see Section 5.3.4) that he is not sideslipping.

(d) Flight with asymmetric thrust and sideslip towards live engine. Sketch 5.3 shows the forces acting in the general case of trimmed flight with both sideslip (towards the live engine) and bank (live engine down). The direction of sideslip is beneficial here since the contributions to sideforce (and hence to the moment countering the effects of thrust asymmetry) due to both the fin and the deflected rudder act in the same direction (and not in opposition, as in cases (a) and (g) – see Sketches 5.1 and 5.5). Zero resultant side force on the aircraft is achieved by balancing the contribution due to the fin, rudder and airframe by the side component of wing lift, produced by banking the live-engine wing down. This class of flight condition is of particular value in cases where the rudder control available is limited.

(e) Flight with rudder central. The forces acting are shown in Sketch 5.4. In this case, which can be seen as a unique example of case (d) (Sketch 5.3), the aeroplane sideslips towards the live engine until the yawing

moment so produced (depending on N_v) balances the moment due to asymmetric thrust. The resulting side force (depending on Y_v) is balanced by the side component of the wing lift produced by banking the live-engine wing down. The angles of bank and sideslip are now considerable.

(f) Flight with rudder free*. If the rudder is balanced by a horn and thus has a tendency to 'float' against the wind, the condition of flight with rudder free will lie between (c) and (e), but if the rudder is balanced by, for example, a geared tab, angles of bank and sideslip even greater than the condition (e) will be needed before the rudder hinge moment becomes zero. This condition of flight would not usually be chosen by the pilot for steady flight because of the large angles of bank and sideslip involved. It is a condition in which fin stall may occur.

(g) Flight with asymmetric thrust with dead engine down. Starting from the first condition mentioned, *i.e.* with wings level, the aeroplane can be flown with the dead engine banked down. This condition is unlikely to be chosen in straight flight because of the large angle of sideslip toward the dead engine and a large rudder angle will be needed to prevent yaw, see Sketch 5.5. This is a condition under which fin stall and rudder overbalance* are prone to occur.

5.2 Wind-Tunnel Data

Wind-tunnel test programmes often include data relevant to the estimation of asymmetric trim drag, for example, sideforce and yawing and rolling characteristics are measured as part of the overall work on stability and control derivatives. Tests to establish the variation of drag coefficient with sideslip and rudder angles are usually conducted for a selection of airframe configurations and angles of attack (and may include "fin-on" and "fin-off" cases) – a typical set of results is shown in Appendix B.

Appendix B demonstrates the use of the data in Sketch B4.2 to estimate the change in aeroplane drag coefficient for particular asymmetric flight cases. The accuracy of this approach depends on how representative the wind-tunnel tests are of flight conditions. Features that may not be represented in the former include aileron and/or spoiler deflections, cowl spillage and powerplant scrubbing or slipstream flows. In addition, the effects of sideslip, on transition, and the various corrections to measured forces and moments, may be less well established than for symmetric configurations.

5.3 Flight-Test Data

There are several approaches to the use of flight tests to measure (or to confirm estimates of) drag due to thrust or airframe asymmetry† and these are considered separately in Sections 5.3.1 to 5.3.3. Where the objective is to measure the drag increment due to thrust asymmetry for a particular aeroplane, results are frequently presented as in Sketch 5.6. Other forms include: substitution of [equivalent airspeed]^2 for q in the parameter on the horizontal axis or multiplication of that parameter by $[l_p/Sb]$ or by $[l_p/S_F x_F]$ or use of the square of any one of these. All of these forms of presentation permit the inclusion of values of $\Delta C_{D_{asym\ thr}}$ from tests made for either or both of the following

(i) for a wide range of flight conditions (and hence q) but a limited range of power settings, for example with one engine windmilling and the other at "climb" power,

(ii) for a wide range of asymmetric thrusts, using differential power settings, but possibly for a limited range of values of q.

A characteristic of presentations such as Sketch 5.6 is that test results obtained at high speeds tend to be concentrated near the origin (especially if the parameter on the horizontal axis is squared). If test data are

* This case is only relevant if the control circuit is such that, "rudder free" implies that rudder position is determined solely by the aerodynamic moment acting.

† Section 5.3 is written in terms of thrust asymmetry. However the same techniques apply for other forms of asymmetry.

obtained at low speeds only, the subsequent extrapolation to the origin (broken line in Sketch 5.6), can, seemingly, provide estimates for much higher-speed conditions but, in practice, test data at higher speeds are more likely to be as indicated by the solid line in the Sketch. This tendency is followed in the presentation of mean lines in Figure 1 and 2.

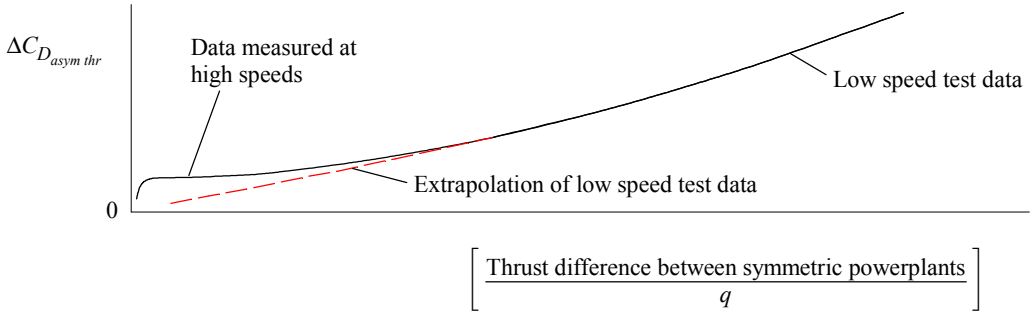

Sketch 5.6 Example of presentation of measured drag coefficient increment due to thrust asymmetry (windmilling drag excluded)

5.3.1 General approach to drag measurement

If time and resources are available, the best method of determining drag due to asymmetry is as part of the overall programme of drag measurement. Data Item No. 79018 (Reference 6) provides an example of the application of three techniques, each involving determination of the resultant acceleration of the aeroplane and the subsequent calculation of lift and drag from a knowledge of engine thrust. In that Item,

(i) Section 4 considers the use of air data measurements only to determine acceleration,
(ii) Section 5 considers the use of body-axis-aligned accelerometers,
(iii) Section 6 considers the use of accelerations derived from an inertial platform.

To apply these methods to determine drag due to thrust asymmetry, the thrust of each engine must be represented separately (in the case of (i), where air-path-axes are used, the force components due to individual engines are given in Section 4.1 of that Item).

5.3.2 Use of climb performance tests to determine drag

Climb performance tests, for example at fixed calibrated airspeed but with one engine at reduced power, or shut down, can be used to deduce the change in drag from that in symmetric flight. Such tests can also be used to confirm pre-flight estimates.

For still air, or for conditions where wind speed does not vary with height, the rate of climb, $\mathrm{d}H/\mathrm{d}t$, is calculated from the along-flight-path equation of motion expressed in the following general form,

$$\frac{\mathrm{d}H}{\mathrm{d}t} = \frac{V}{W}\frac{[\text{component of thrust along airspeed vector minus drag}]}{\left[1 + \frac{V}{g_0}\frac{\mathrm{d}V}{\mathrm{d}H}\right]}. \qquad (5.1)$$

A derivation and detailed presentation of Equation (5.1) is given in Item No. 70023 (Reference 5) together with additional information on test techniques *etc*. For known flight conditions, *i.e*. climb technique, speed, weight and thrusts, changes in airframe drag for different levels of thrust asymmetry can be deduced from measured values of climb rate using Equation (5.1). Values of the acceleration factor (the term in square brackets in Equation (5.1)) are given in Item No. 81046 (Reference 7) for climbs at constant equivalent airspeed, constant calibrated airspeed and constant Mach number.

5.3.3 Combined use of flight-test and wind-tunnel data

If wind-tunnel data are available (and assuming that all significant effects of asymmetry are correctly modelled), initial flight tests may be limited to determining the combinations of sideslip and rudder deflection angles corresponding to steady, straight trimmed flight. Values of ΔC_D can then be deduced directly from the wind-tunnel data and, if required, bank angles can be determined using Equation (4.12). The values of ΔC_D so obtained can be validated by using them to estimate climb performance with an inoperative engine and checking these against actual climb performance (see Section 5.3.2). Such validation would be essential for civil certification.

5.3.4 Limitations

Drag due to asymmetry is a (relatively) small difference between drags in symmetric and asymmetric flight conditions and so is inevitably a difficult quantity to measure accurately. A major difficulty is the establishment of steady, repeatable test conditions and in this respect the use of climb tests (Section 5.3.2) introduces further uncertainties. If rudder deflection and sideslip angles are measured, then some of the apparent scatter in flight-derived data (when plotted as in Sketch 5.6) can be explained. Measurements of ζ and β are, of course, essential to the technique of Section 5.3.3. The repeatability of results can also be enhanced by restricting the range of flight techniques and control inputs used.

One such technique is to avoid all use of roll controls ("centralised roll controls"), use the minimum rudder deflection required to counter the yawing moment due to thrust asymmetry and accept the resulting combination of sideslip and bank angles. This technique is widely used with jet- and fan-engined transports and leads to a relatively low level of drag due to asymmetry. It is, of course, particularly beneficial if use of lateral controls would result in spoiler deployment. Other, less practicable, methods of limiting the range of possibilities are as follows.

(i) To aim for flight at zero sideslip; this is desirable since it corresponds to low drag, see Sketches 4.1 and B4.2, but is difficult to establish without special instrumentation, for example, a head-up display with appropriate air-data inputs. The ability to reproduce, operationally, what had been demonstrated in flight test, would also have to be established.

(ii) To fly with zero rudder deflection; this is a high drag configuration and involves large bank angles so that it is of little practical value.

Analysis of test data requires a knowledge of the asymmetric forces imposed on the aeroplane,

(i) to calculate values of the imposed moment, see Section 4.2.1,

(ii) to deduce aeroplane drag using the methods described in Section 5.3.

In a detailed analysis to deduce airframe drag, a system of thrust and drag accounting is essential and values are required for windmilling drag, cowl spillage drag and for any drag or lift changes associated with changes in slipstream and scrubbing flows. It is possible that for some installations values of windmilling drag and of thrust at low power settings may be less well established than at higher settings and estimates may not be available for all the other powerplant-related force components. One frequent result is that the value of "drag due to asymmetry" often includes other terms. For example, in deriving the method of Section 3 and Figures 1 and 2, it was found that for most of the available data, the quoted value of $\Delta C_{D_{asym\ thr}}$ included all drag components (due to asymmetry) except for the engine manufacturer's quoted windmilling drag.

The scatter on the measured data for any one aircraft can be large. Of two aircraft flying with wings level one exhibited a scatter of ± 0.01 on a range of $\Delta C_{D_{asym\ thr}}$ from 0 to 0.02 and the other exhibited a scatter of ± 0.005 on a range of values from 0 to 0.014. Somewhat better repeatability and hence lower scatter of measured data is found with the "roll controls centralised" technique.

6. ESTIMATION OF INDIVIDUAL DRAG COMPONENTS

Significant drag components associated with methods of countering yawing and rolling moments due to asymmetry in thrust or airframe configuration are as follows (the list is not exhaustive).

Fin and rudder induced drag due to the sideforce required to counter a yawing moment, see Section 6.1,

Fin and rudder profile drag change due to rudder deflection, see Section 6.2,

Airframe (fin-off) drag due to sideslip, see Section 6.3,

Wing induced drag changes due to change in lift distribution associated with:
aileron and/or spoiler deployment to counter any rolling moment,
aircraft sideslip,
changes in engine exhaust or propeller slipstream flows,

Change in profile drag due to aileron deflection, see Section 6.4,

Spoiler profile drag, see Section 6.5,

Change in profile drag due to changes in extent to which airframe components are immersed in propeller slipstream or engine scrubbing flows,

Interference of cowl separated spill flow with other airframe components.

In addition, the yawing moment due to aileron/spoiler deployment and rolling moment due to fin and rudder sideforce will, if present, modify the imposed moments due to asymmetry.

6.1 Fin and Rudder Sideforce and Induced Drag

From Appendix A, Equation (A1.2), the value of fin and rudder sideforce coefficient, C_{Y_F}, needed to counter a yawing moment, N_{asym}, due to asymmetry, is

$$C_{Y_F} = \frac{Y_F}{qS_F} = \frac{N_{asym}}{qS_F x_F}. \tag{6.1}$$

Expressions for N_{asym} may be derived to suit the particular forces involved – see Section 4.2.1.

The fin and rudder induced drag may be expressed in coefficient form (based on fin area) as,

$$C_{D_{F,ind}} = \frac{D_{F,ind}}{qS_F}, \tag{6.2}$$

and values may be converted to the corresponding contribution to aeroplane drag coefficient using,

$$(\Delta C_D)_{F,ind} = C_{D_{F,ind}} \times \frac{S_F}{S}. \tag{6.3}$$

The relationship between $\Delta(C_D)_{F,ind}$ and N_{asym} for the case of steady straight flight with a yawing moment due to asymmetry is derived in Section A2 of Appendix A – see Equation (A2.4). A method for adapting Equation (A2.4) to multiple-fin configurations is given in Section A2.3.

Methods of estimating the fin and rudder sideforce and induced drag are discussed in Sections 6.1.1 and 6.1.2.

6.1.1 Estimation of fin sideforce

The method, using two Items from the Aerodynamics Series, is as follows.

Data Item in Aerodynamics Series		Method
No.	Title	
70011 Ref. 9	Lift-curve slope and aerodynamic centre position of wings in inviscid subsonic flow.	Figure 1 of Item is used to deduce lift-curve slope (there denoted $dC_L/d\alpha$) for straight-tapered "wing" of aspect ratio $A_F(=2h_F^2/S_F)$, taper ratio c_{t_F}/c_{r_F}, half-chord sweep angle $\Lambda_{½F}$, and area $2S_F$.
82010 Ref. 13	Contribution of fin to sideforce, yawing moment and rolling moment derivatives due to sideslip, $(Y_v)_F$, $(N_v)_F$, $(L_v)_F$ in the presence of body, wing and tailplane.	Values of lift-curve slope from Item No. 70011, denoted $(C_{L\alpha})_F$ here and in Item No. 82010, are converted into values of the fin contribution, $(Y_v)_F$, to the sideforce derivative due to sideslip using, $(Y_v)_F = -J_B J_T J_W (C_{L\alpha})_F S_F/S$, where J_B, J_T, J_W are factors to account for body, tail location and wing location (values of J_B, J_T, J_W are presented in Figures 1, 2, 3 of the Item).

6.1.2 Estimation of fin induced drag

There is no separate Data Item dealing with this topic. However, to a first approximation, values may be estimated using the following relationship which is based on the method of estimating $(Y_v)_F$ described in Section 6.1.1 but with the factor $J_W = 1$. The contribution to aeroplane drag coefficient due to fin induced drag is given by

$$(\Delta C_D)_{F,ind} = \frac{0.8}{\pi A_F}\left[J_B J_T (C_{L_a})_F \frac{\beta\pi}{180}\right]^2 \frac{S_F}{S}. \qquad (6.4)$$

The method of Equation (6.4) is valid for fully attached flow only and in any event should be restricted to $\beta < 10$ deg. The underlying method of Item No. 82010 for $(Y_v)_F$ is itself based on experimental data over small ranges of sideslip angles about zero, typically between ± 2 and ± 5 deg.

Comparison of results from Equation (6.4) with "measured" values deduced from wind-tunnel tests with ten models (see Reference 35) suggests that the results should be within ± 30 per cent as long as attached flow conditions prevail. The "measured" values used in these comparisons were deduced as follows.

(i) For each test where both "fin-on" and "fin-off" measurements of C_D were available as functions of β, the quantities $\{[C_D]-[C_D]_{\beta=0}\}_{FIN\ ON}$ and $\{[C_D]-[C_D]_{\beta=0}\}_{FIN\ OFF}$ were deduced, *i.e.* differences between the value of C_D at $\beta = 0$ and the value at each finite value of β.

(ii) "Measured" values of the fin-induced contribution to drag coefficient were deduced as

$$\{[C_D] - [C_D]_{\beta=0}\}_{FIN\ ON} - \{[C_D] - [C_D]_{\beta=0}\}_{FIN\ OFF}. \qquad (6.5)$$

6.2 Fin and Rudder Profile Drag

Figure 4 gives a method for estimating the change in fin and rudder profile drag due to a known rudder deflection angle. The Figure is adapted from Aerodynamics Item No. 87024 (Reference 21) but includes an indication of the spread of the source data.

Values of the drag parameter given in Figure 4 are converted to the corresponding contribution to aeroplane drag coefficient, $(\Delta C_D)_{F,profile}$ using

$$(\Delta C_D)_{F,profile} = \left[\frac{(D_F - D_{F_{\zeta=0}})_{profile}}{qS_R}\right] \times \frac{S_R}{S}. \tag{6.6}$$

A complete calculation process, including the estimation of rudder angle to give the required fin and rudder sideforce, would include the method described in Section 6.1.1 and would then continue as follows.

Data Item in Aerodynamics Series		Method
No.	Title	
87008 Ref. 14	Rudder sideforce, yawing moment and rolling moment control derivatives at low speeds: Y_ζ, N_ζ and L_ζ.	Method applies plain-control effectiveness parameter to modified form of fin sideforce derivative (see Section 6.1.1) to obtain rudder derivatives. Hence deduce rudder deflection, ζ, to give required sideforce coefficient as function of sideslip angle, β.
87024 Ref. 21	Low speed drag coefficient increment at constant lift due to full-span plain flaps.	Figure 1 of Item No. 87024 (main carpet) gives drag coefficient of fin and rudder as function of rudder to fin chord ratio and rudder deflection angle. Figure 4 in present Item is derived from that Figure.

6.3 Airframe Drag Due to Sideslip (Fin-Off)

Figure 5 gives a guide to the increase in fin-off airframe drag coefficient, due to change in sideslip angle β. The figure is based on low speed wind-tunnel data (see Reference 35) for eleven aeroplane models (fin-off) together with data for tests on several fuselages and two airships (fins-off). Most of the data were for models with circular-cross-section fuselages/bodies but a limited amount of data is included for elliptic and "double-bubble" shapes.

Values of the drag parameter given in Figure 5 are converted to the corresponding contribution to aeroplane drag coefficient, $\Delta C_{D_{sideslip}}$, using

$$\Delta C_{D_{sideslip}} = \left[\frac{[D - D_{\beta=0}]_{sideslip}}{qh_B^2}\right] \times \frac{h_B^2}{S}. \tag{6.7}$$

6.4 Aileron Drag

Ailerons contribute only a small component of total drag due to asymmetry, see Sketch 4.1.

There is no method in the ESDU Aerodynamic Series for estimating the induced drag due to aileron deflection. However, Item No. Flaps 02.01.08 provides a method for estimating the vortex drag of a wing with symmetrically deployed part-span flaps. As a first approximation it is suggested that the change in induced drag due to aileron deflection at constant lift may be obtained from the second term of Equation (2.1) of that Item with the incremental lift coefficient taken as,

$$\text{incremental lift coefficient, } \Delta C_L = \frac{L_{asym}}{qSy_{aileron}}, \tag{6.8}$$

where L_{asym} is the imposed rolling moment due to asymmetry and $y_{aileron}$ is the coordinate of the aileron mid-span point. An alternative approach is given in Reference 24.

Aileron profile drag changes can be estimated as follows. Data Item No. 88013 (Reference 22) can be used to predict aileron deflection angle for given value of L_{asym}; Item No. 87024 (Reference 21) can then be used to deduce the profile drag increment (full-span controls) and Item No. F.02.01.07 (Reference 15) used as a correction to part span.

6.5 Spoiler Drag

If spoiler controls act with ailerons, their contribution to drag can be considerable, see Sketch 4.1. Estimates of the profile drag penalty incurred for a given change in lift can be made using Figure 6 which has been generated using information from four Items in the Aerodynamics Series, as follows.

Data Item in Aerodynamics Series		Method
No.	Title	
74009 Ref. 17	Lift coefficient increment at low speeds due to full-span split flaps.	The data from these two Items have been combined to form Figure 6b in the present Data Item.
74010 Ref. 18	Low-speed drag coefficient increment at zero lift due to full-span split flaps.	
74012 Ref. 20	Conversion of lift coefficient increment due to flaps from full span to part span.	Data from Item No. 74012 are presented as Figure 6a in the present Item and should be used before reading values from Figure 6b.
Flaps 02.01.07 Ref. 15	Conversion factor for profile drag increment for part-span flaps.	Data from Item No. Flaps 02.01.07 are presented as Figure 6c in the present Item and should be used to adjust values of ΔC_D obtained from Figure 6b.

7. REFERENCES

7.1 Data Items on Drag Estimation for Inoperative Powerplants

1. ESDU — Approximate estimation of drag of windmilling propellers. ESDU **Performance** Data Item No. ED1/1, April 1962.

2. ESDU — Estimation of windmilling drag and airflow of turbo-jet and turbo-fan engines. ESDU **Performance** Data Item No. 81009, June 1981 (with Amendment A, April 1984).

3. ESDU — Estimation of spillage drag for a wide range of axisymmetric intakes at $M < 1$. ESDU **Performance** Data Item No. 84004, April 1984 (with Amendment A, June 1984).

4. ESDU — Estimation of drag due to inoperative turbo-jet and turbo-fan engines using Data Item Nos 81009 and 84004. ESDU **Performance** Data Item No. 84005, July 1984.

7.2 Other Relevant Data Items in Performance Series

5. ESDU — The measurement and analysis of climb performance. ESDU **Performance** Item No. 70023, September 1970 (with Amend. A, June 1982).

6. ESDU — Example of performance analysis using data obtained concurrently in air-path, body and Earth axes. ESDU **Performance** Item No. 79018, November 1979.

7. ESDU — Acceleration factors for climb and descent rates at constant EAS, CAS, M. ESDU **Performance** Item No. 81046, November 1981.

8. ESDU — Force and moment components for take-off and landing calculations. ESDU **Performance** Item No. 85030, November 1985.

7.3 Data Items on Estimation of Wing Lift and Induced Drag (with Applications to Fins)

9. ESDU — Lift-curve slope and aerodynamic centre position of wings in inviscid subsonic flow. ESDU **Aerodynamics** Item No. 70011, July 1970 (with Amend. C, July 1977).

10. ESDU — Subsonic lift-dependent drag due to trailing vortex wake for wings without camber or twist. ESDU **Aerodynamics** Item No. 74035, October 1974.

7.4 Data Items on Estimation of Fin and Rudder Lift and Induced Drag

11. ESDU — Lift-curve slope, for single fin and rudder. (i) Body shape merging into fin. ESDU **Aerodynamics** Item No. C.01.01.01, January 1955 (with Amend. B, April 1982).

12. ESDU — Lift-curve slope for twin fins and rudders. ESDU **Aerodynamics** Item No. C.01.01.02, March 1955 (with Amend. B, April 1982).

13. ESDU — Contribution of fin to sideforce, yawing moment and rolling moment derivatives due to sideslip, $(Y_v)_F$, $(N_V)_F$, $(L_v)_F$ in the presence of body, wing and tailplane. ESDU **Aerodynamics** Item No. 82010, April 1982 (with Amend. B, March 1987).

14. ESDU — Rudder sideforce, yawing moment and rolling moment control derivatives at low speeds; Y_ζ, N_ζ and L_ζ. ESDU **Aerodynamics** Item No. 87008, June 1987.

7.5 Data Items on Estimation of Lift and Drag of Controls and Flaps

15. ESDU — Conversion factor for profile drag increment for part-span flaps. ESDU **Aerodynamics** Item No. F.02.01.07, June 1944 (with Amend. B, July 1974).

16. ESDU — Vortex drag coefficient of wing with part-span flap and central cut-out. ESDU **Aerodynamics** Item No. F.02.01.08, April 1945 (with Amend. B, May 1981).

17. ESDU — Lift coefficient increment at low speeds due to full-span split flaps. ESDU **Aerodynamics** Item No. 74009, May 1974.

18. ESDU — Low-speed drag coefficient increment at zero lift due to full-span split flaps. ESDU **Aerodynamics** Item No. 74010, July 1974 (with Amend. A, November 1974).

19. ESDU — Rate of change of lift coefficient with control deflection for full-span plain controls. ESDU **Aerodynamics** Item No. 74011 July 1974.

20. ESDU — Conversion of lift coefficient increment due to flaps from full span to part span. ESDU **Aerodynamics** Item No. 74012, July 1974 (with Amend. A, February 1985).

21. ESDU — Low-speed drag coefficient increment at constant lift due to full-span plain flaps. ESDU **Aerodynamics** Item No. 87024, December 1987.

22. ESDU — Rolling moment derivative, L_{ξ}, for plain ailerons at subsonic speeds. ESDU **Aerodynamics** Item No. 88013, August 1988.

7.6 Other References

23. DOUGLAS, D.W. — The developments and reliability of the modern multi-engine air liner with special reference to multi-engine airplanes after engine failure. J. Aeronaut. Sci., Vol. 2, No. 4, July 1935.

24. PEARSON, H.A. — Theoretical span loading and moments of tapered wings produced by aileron deflection. NACA tech. Note 589, November 1935.

25. HARTMAN, E.P. — Wind-tunnel tests of a 2-engine airplane model as a preliminary study of flight conditions arising on the failure of one engine. NACA tech. Note 646, March 1938.

26. JOHNSON, C.L. — Rudder control problems on four-engined airplanes. SAE Journal (Transactions), Vol. 46, No. 6, June 1940.

27. YATES, A.H. — Control in flight under asymmetric power. Aircraft Engineering, Vol. 19, No. 223, September 1947.

28. WRIGHT, I.E. — Flight on asymmetric engine power. Aircraft Engineering, Vol. 22, No. 262, December 1950.

29. ALLCROFT, J. — Yaw drag. HSA (Hat) Aero. Dept./5929/JA/GEN (unpublished work at HSA, Hatfield), 1967.

30. GALLAY, M.L. — Flight of aircraft with partial and unbalanced thrust. NASA TT F-734, April 1973.

31. CALLAGHAN, J.G. — Aerodynamic prediction methods for aircraft at low speeds with mechanical high lift devices. In, Prediction methods for aircraft aerodynamic characteristics, AGARD Lecture Series 67, May 1974.

32. WANNER, J.C. — Dynamique du vol et pilotage des avions. ONERA Publication No. 1976-6, 1976.

33. ESDU — Introduction to aerodynamic derivatives, equations of motion and stability. ESDU **Aerodynamics** Item No. 86021, October 1986, (with Amend. A, March 1987).

34. ZONDERVAN, P.R. — The minimum control speed (V_{MCA}) and the asymmetric trim drag during take-off climb for turbine-powered airplanes. Delft University, Faculty of Aerospace Engineering, July 1987.

35. MITCHELL, D.J. — Summary of work in support of ESDU Data Item No. 88006, "Estimation of drag arising from asymmetry in thrust or airframe configuration". ESDU Memor. No. 67, November 1988 (supersedes ESDU Memor. No. 57, July 1985).

8. EXAMPLE OF USE OF FIGURES 1 AND 2

Use the methods of Figures 1 and 2 to estimate the change in drag coefficient due to thrust asymmetry for the turbo-fan engined aeroplane described in Section B1 of Appendix B. Estimate values for both "roll controls centralised" and "wings level" flight conditions for the following case ("case (i)" in Appendix B),

$$W = 175\,000 \text{ lbf}, \quad V = 143 \text{ kn}, \quad 241.4 \text{ ft/s}, \quad M = 0.2162, \quad q = 69.2465 \text{ lbf/ft}^2.$$

From Appendix B, Section B1.1, $S = 1400 \text{ ft}^2$, $l_F (\approx x_F) = 60$ ft, $h_F = 20$ ft.

For use with Figure 2, assume $h_B = 15$ ft.

For this class of aeroplane, Section 3 suggests that the parameter used in Figures 1 and 2 be expressed in the form

$$\frac{1}{2\pi}\left(\frac{N_{asym}}{q}\right)^2\left(\frac{1}{l_F h_F}\right)^2\frac{1}{S} = \frac{1}{2\pi}\left(\frac{F_N + D_{wm}}{q}\right)^2\left(\frac{l_p}{l_F h_F}\right)^2\frac{1}{S}.$$

For $M = 0.2162$, Sketch B4.1 gives $F_N = 20\,950$ lbf, from which the value of $N_{asym} = 404\,181$ lbf ft is deduced in Section B2. The corresponding value of the parameter used in Figures 1 and 2 is

$$\frac{1}{2\pi}\left(\frac{404\,181}{69.2465}\right)^2\left(\frac{1}{20 \times 60}\right)^2\frac{1}{1400} = 0.002\,69.$$

For this value of the parameter on the horizontal axis in Figure 1, the mean line provides an estimate for "roll controls centralised", of

$$\Delta C_{D_{asym\ thr}} = 0.0065.$$

For the value of 0.002 69 for the parameter on the horizontal axis of Figure 2 and, from given information, for $(h_F/h_B)^2 = (20/15)^2 = 1.778$, this Figure provides an estimate for "wings level", of

$$\Delta C_{D_{asym\ thr}} = 0.0138.$$

These values of $\Delta C_{D_{asym\ thr}}$ may be compared with values estimated for case (i) in Appendix B (where wind-tunnel data are used to predict the effects of rudder and sideslip angles on airframe drag) as follows.

From Section B4, the minimum increment in drag coefficient ≈ 0.006.

From the Table in Section B3.1, the increment in drag coefficient for flight with wings level ($\Phi = 0$) $= 0.0114$.

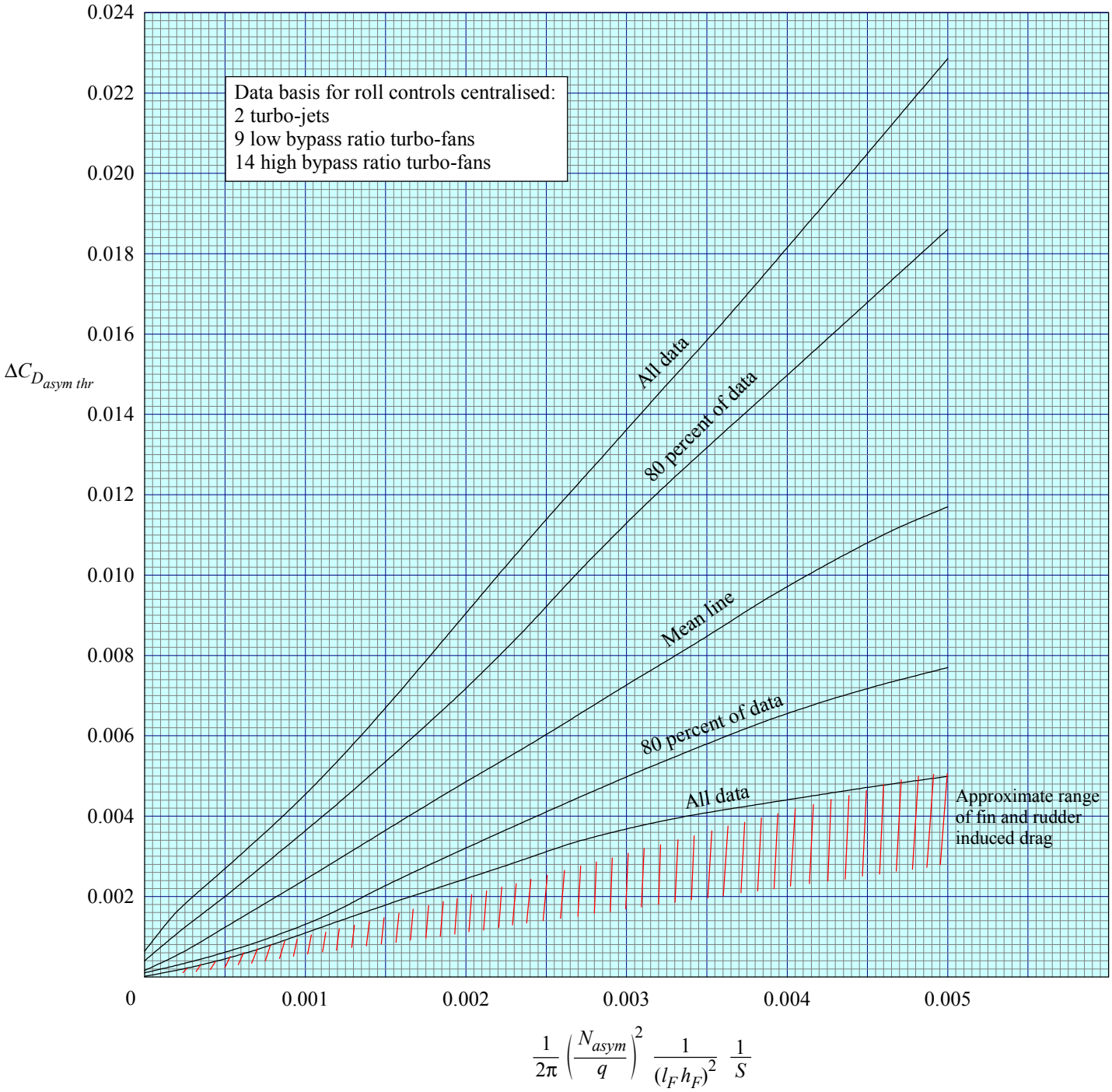

FIGURE 1 INCREMENT IN DRAG COEFFICIENT DUE TO THRUST ASYMMETRY: JET- AND FAN-ENGINED AEROPLANES WITH ROLL CONTROLS CENTRALISED

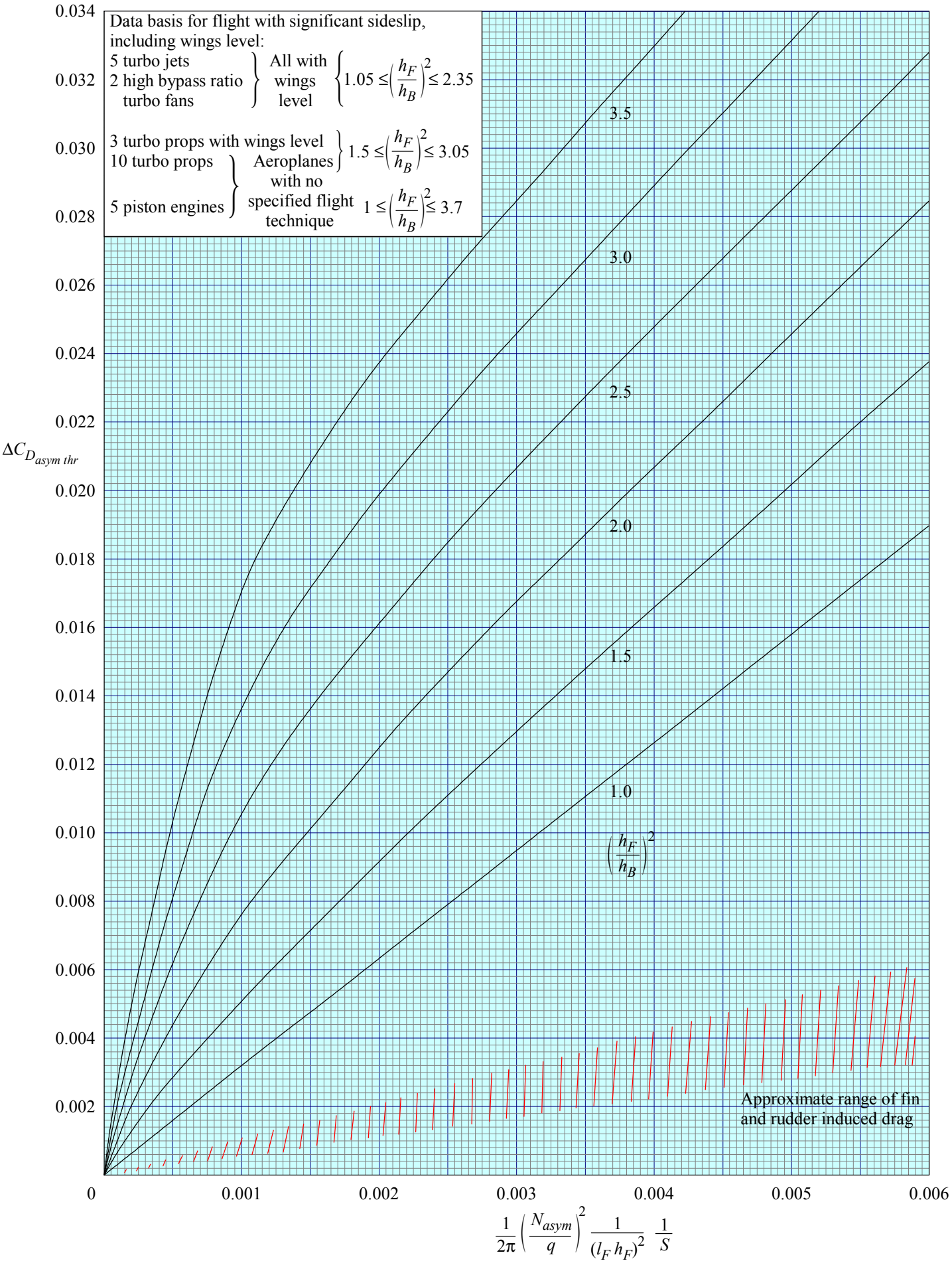

FIGURE 2 INCREMENT IN DRAG COEFFICIENT DUE TO THRUST ASYMMETRY: FLIGHT WITH SIGNIFICANT SIDESLIP, INCLUDING WINGS LEVEL

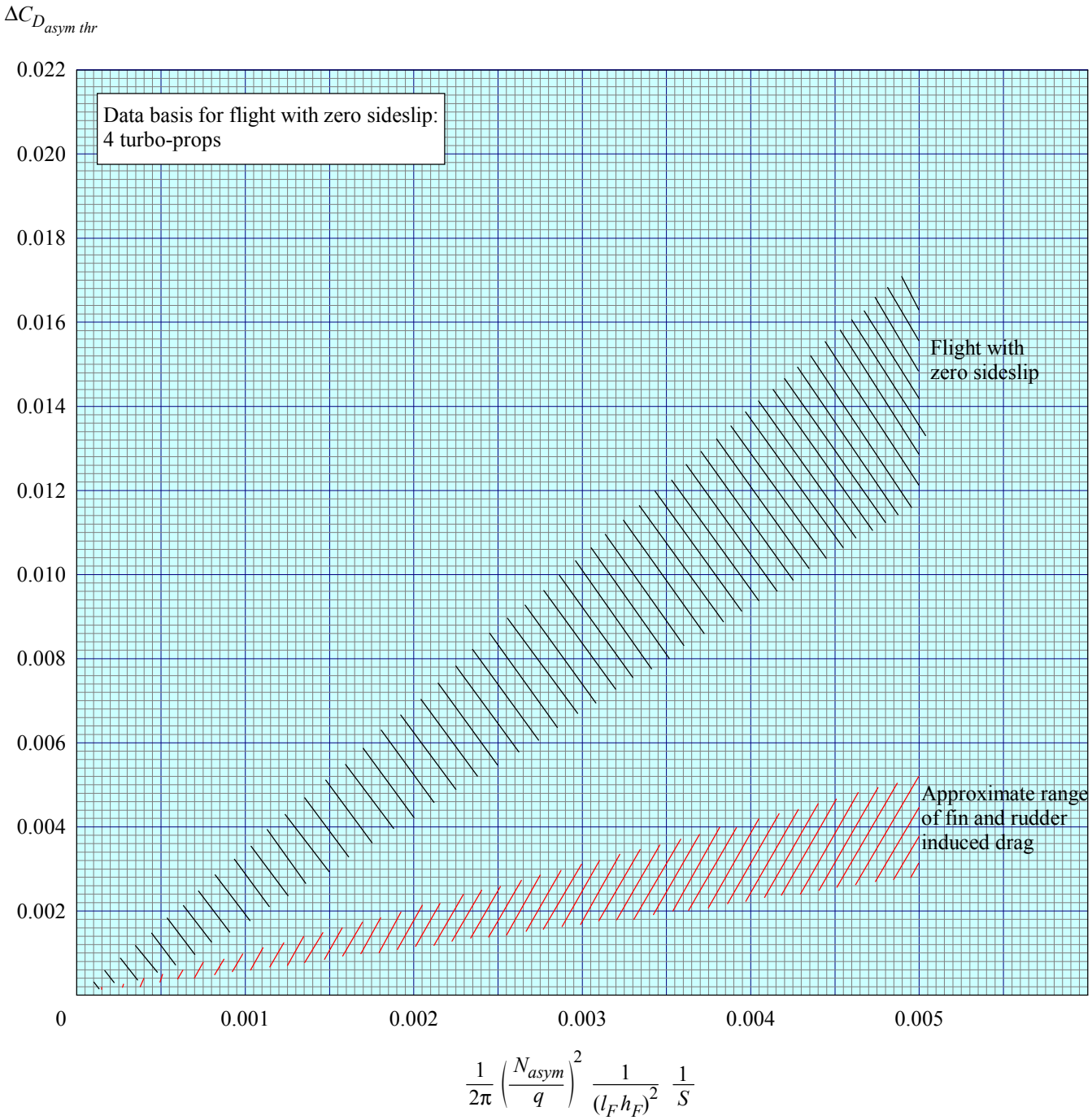

FIGURE 3 INCREMENT IN DRAG COEFFICIENT DUE TO THRUST ASYMMETRY: PROPELLER-DRIVEN AEROPLANES WITH ZERO SIDESLIP

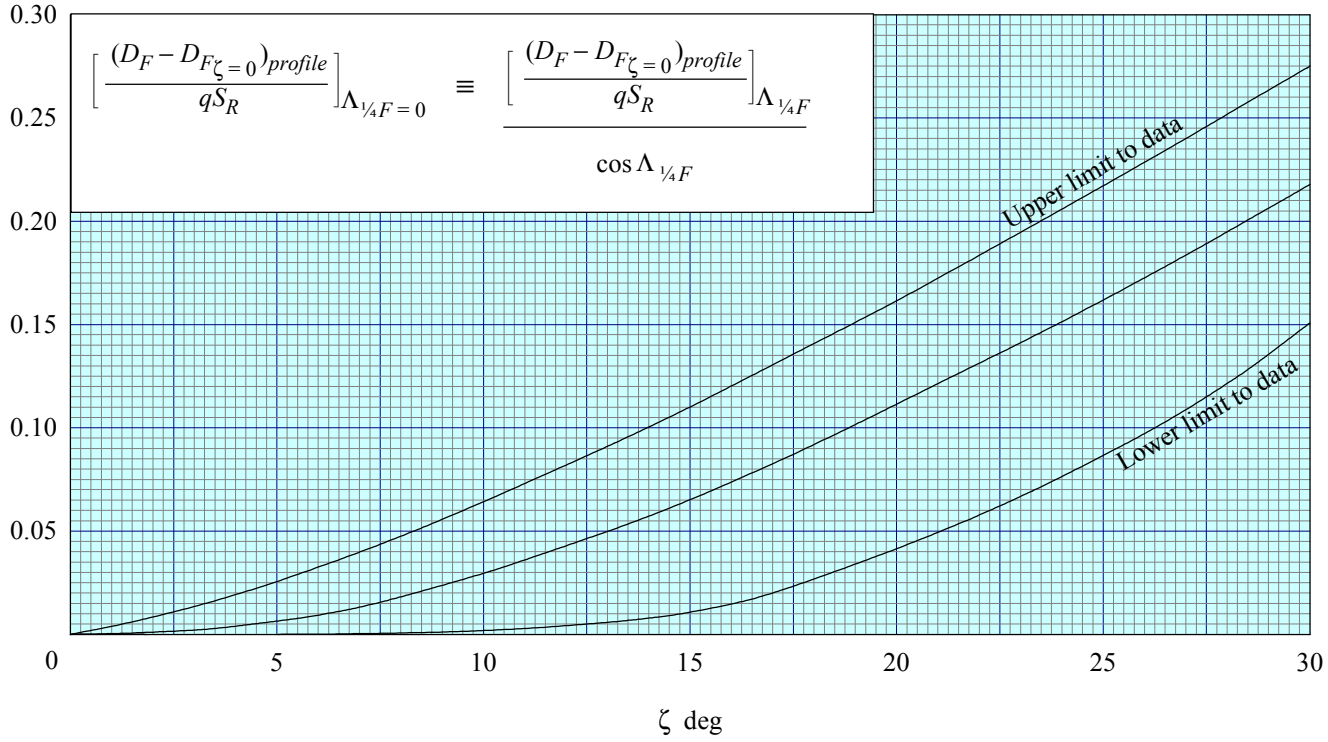

FIGURE 4 PROFILE DRAG INCREMENT OF FIN AND RUDDER DUE TO RUDDER DEFLECTION (FULL SPAN) (See Section 6.2 for basis)

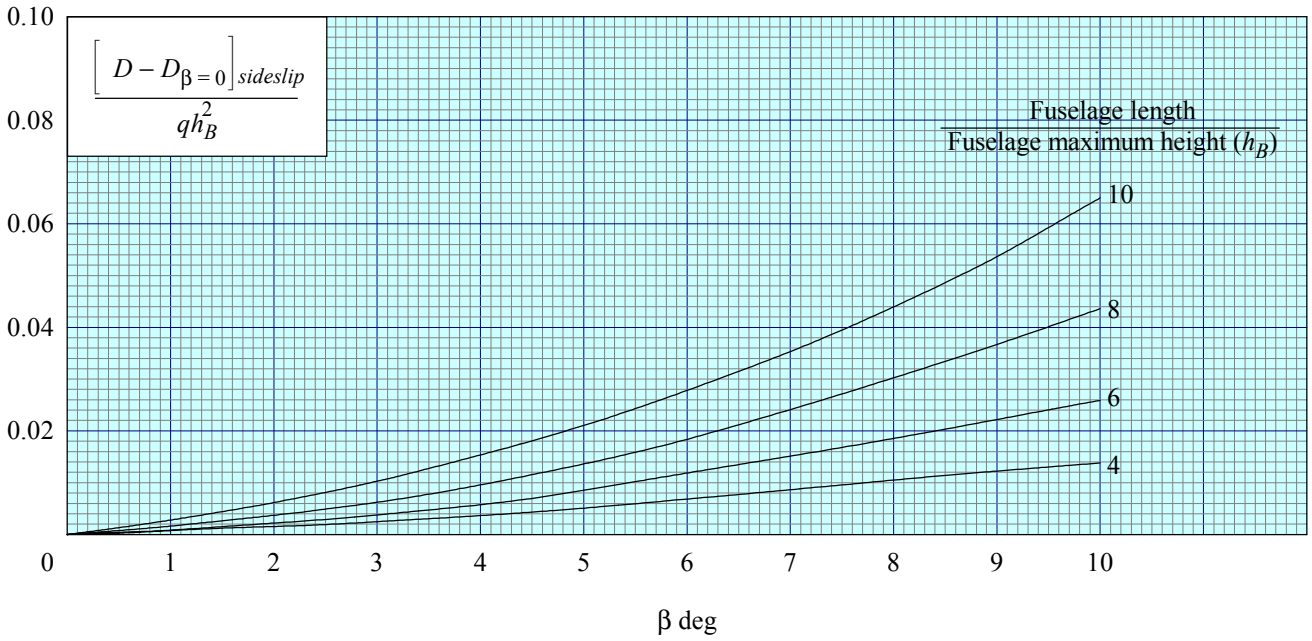

FIGURE 5 EFFECT OF SIDESLIP ON AEROPLANE DRAG (FIN-OFF) (See Section 6.3 for basis)

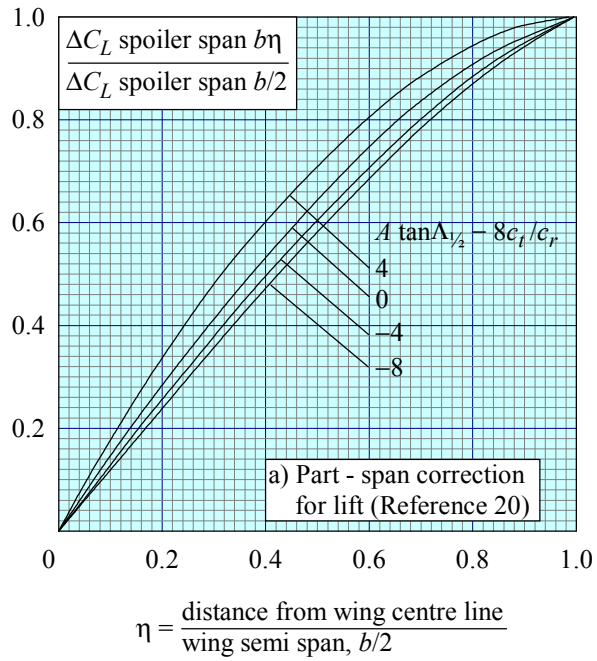

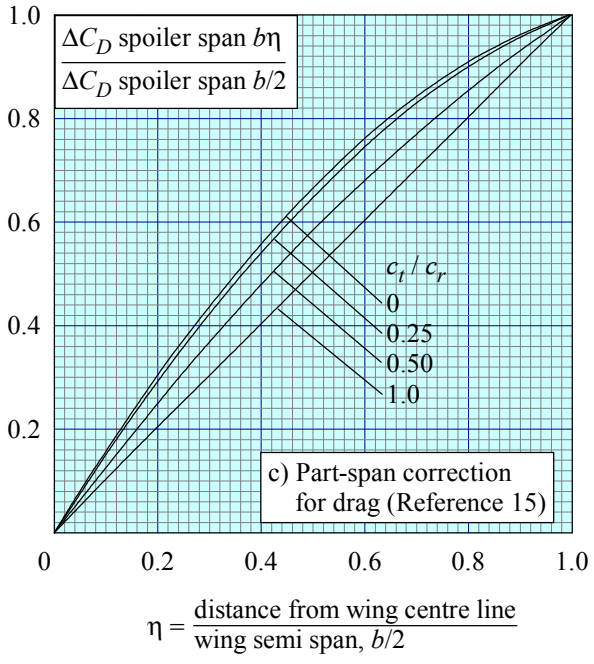

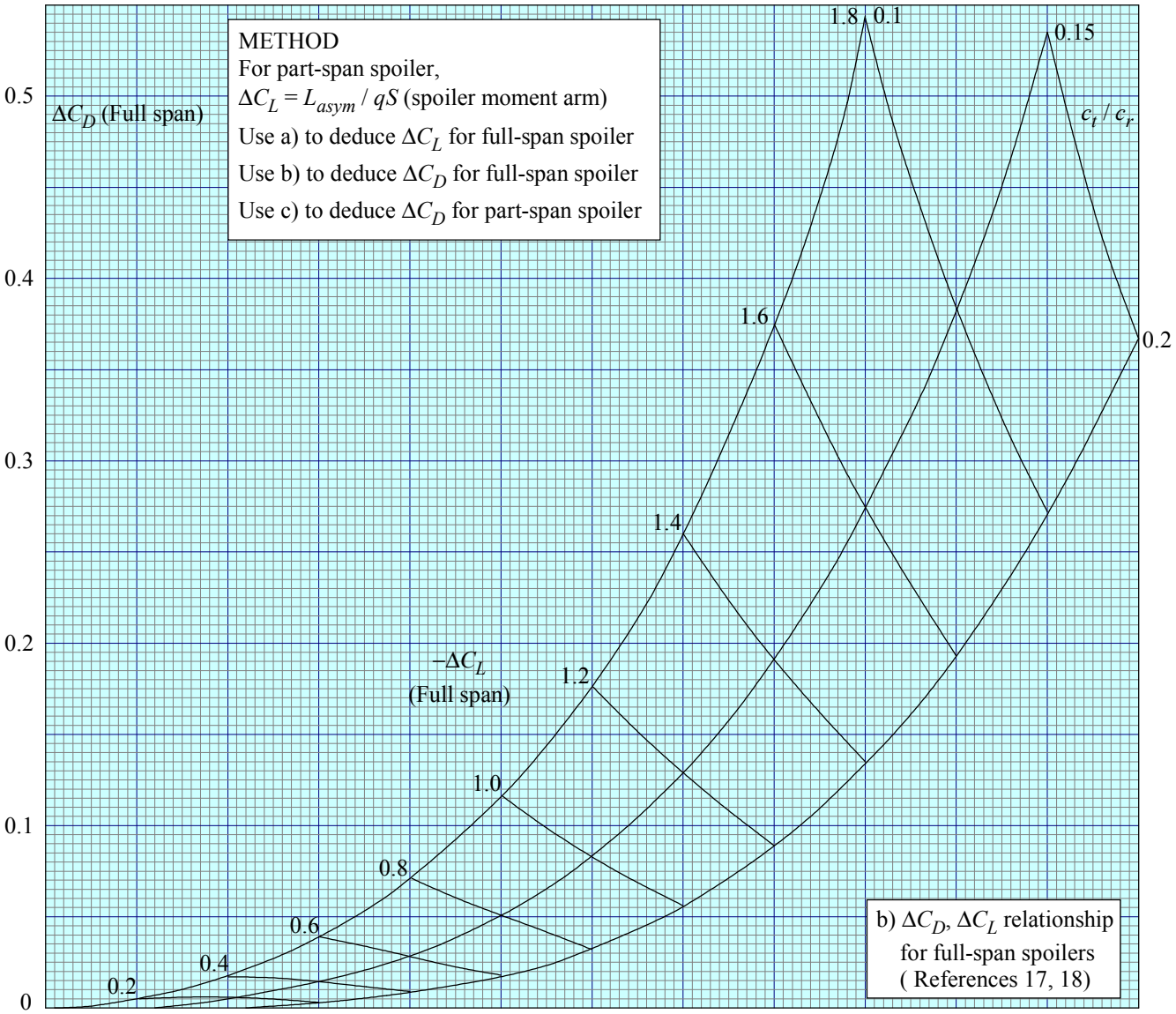

FIGURE 6 ESTIMATION OF SPOILER PROFILE DRAG COEFFICIENT
(See Section 6.5 for basis)

APPENDIX A FIN AND RUDDER SIDEFORCE AND INDUCED DRAG IN STEADY STRAIGHT FLIGHT WITH YAWING MOMENT DUE TO ASYMMETRY IN YAW

A1. FIN AND RUDDER SIDEFORCE

Consider an aeroplane in steady flight but subject to a yawing moment, N_{asym}, due to asymmetry. Assume that this yawing moment is counteracted by a sideforce, Y_F, on the fin and rudder acting at distance x_F from the aeroplane centre of gravity (moment reference point). By equating moments,

$$Y_F = \frac{N_{asym}}{x_F}. \tag{A1.1}$$

This sideforce may be expressed in coefficient form based on fin and rudder area, S_F, as

$$C_{Y_F} = \frac{Y_F}{qS_F} = \frac{N_{asym}}{qS_F x_F}. \tag{A1.2}$$

A2. FIN AND RUDDER INDUCED DRAG

The fin and rudder induced drag coefficient corresponding to C_{Y_F} may be expressed as

$$C_{D_{F,ind}} = \frac{K_F (C_{Y_F})^2}{\pi A_F} \tag{A2.1}$$

where A_F is the aspect ratio of the fin and rudder. For a fin and rudder area, S_F, and height, h_F, and assuming that the fuselage acts as an ideal reflection plane, the fin aspect ratio may be expressed as

$$A_F = \frac{(2h_F)^2}{2\,S_F} = \frac{2\,h_F^2}{S_F}. \tag{A2.2}$$

Substituting from Equations (A1.2) and (A2.2) into Equation (A2.1) gives

$$\begin{aligned} C_{D_{F,ind}} &= \frac{K_F}{\pi}\left[\frac{N_{asym}}{qS_F x_F}\right]^2 \frac{S_F}{2h_F^2} \\ &= \frac{K_F}{2\pi}\left[\frac{N_{asym}}{qx_F}\right]^2 \frac{1}{S_F h_F^2} \end{aligned} \tag{A2.3}$$

If the corresponding contribution to aeroplane drag coefficient, based on wing reference area, S, is denoted $\Delta(C_D)_{F,ind}$, then

$$\Delta(C_D)_{F,ind} = C_{D_{F,ind}} \times \frac{S_F}{S}$$

i.e.

$$(\Delta C_D)_{F,ind} = \frac{K_F}{2\pi}\left[\frac{N_{asym}}{qx_F}\right]^2 \frac{1}{Sh_F^2}. \tag{A2.4}$$

A2.1 Derivation of Parameter Used in Section 3 and Figures 1 and 2

Section 3 of this Item introduces Figures 1 to 3 which present summaries of established data for $\Delta C_{D_{asym\ thr}}$ due to asymmetry in jet- or fan-engine thrust and in propeller thrust. The parameter used for presenting/correlating these data is derived as follows.

(i) The yawing moment due to asymmetric engine or propeller thrusts is assumed to be counteracted by the moment due to fin and rudder sideforce – as given by Equation (A1.2).

(ii) The drag due to asymmetric engine or propeller thrusts is assumed equal to the induced drag corresponding to the fin and rudder sideforce and so is given by Equation (A2.4).

(iii) For ease of calculation, the moment reference point is taken as the aerodynamic centre rather than the aeroplane centre of gravity. Consequently, the fin and rudder moment arm, x_F, in Equation (A2.4) is replaced by the length, l_F, defined in Sketch 3.1.

(iv) The parameter used in Figures 1 to 3 is the right-hand side of Equation (A2.4) with K_F omitted and $x_F = l_F$, *i.e.*

$$\frac{1}{2\pi}\left[\frac{N_{asym}}{q}\right]^2 \frac{1}{l_F^2 h_F^2 S}\ .$$

A2.2 Evaluation of N_{asym}

For a pair of engines located symmetrically at distances l_p from the aeroplane centre line, but operating at different thrusts, the yawing moment due to thrust asymmetry is

$$N_{asym} = (\text{thrust difference between engines})\ l_p\ .$$

For more than one pair of engines, the yawing moment due to thrust asymmetry is

$$N_{asym} = \Sigma\ [(\text{thrust difference between pair of engines})\ l_p\ ].$$

For a pair of jet or fan engines, one operating at net thrust F_N, the other generating windmilling drag D_{wm}, the value of N_{asym} is usually given to a satisfactory approximation by $(F_N + D_{wm})l_p$, while for a symmetrically located pair of propellers N_{asym} is given by $(T + D_{feathered})l_p$ or $(T + D_{wm})l_p$, as appropriate.

Thus, for jet- and fan-engined aeroplanes with one engine inoperative, the parameter derived in Section A2.1 becomes

$$\frac{1}{2\pi}\left[\frac{F_N + D_{wm}}{q}\right]^2 \left[\frac{l_p}{l_F h_F}\right]^2 \frac{1}{S}.$$

Corresponding expressions for propeller-driven aeroplanes are obtained by replacing the term $(F_N + D_{wm})$ by $(T + D_{feathered})$ or $(T + D_{wm})$.

A2.3 Height of Equivalent Single Fin for Multiple-Fin Configurations

Fin height, h_F, in the expressions in Sections A2 and A2.1 is defined in Sketch 1.1 for a single, fuselage-mounted, dorsal fin. An expression is derived here for an "equivalent-single-fin" value of h_F, giving the same fin-induced contribution to aeroplane drag coefficient, as a multiple-fin configuration. The following assumptions are made.

(i) Each vertical (or inclined) surface that extends either above or below a fuselage or tailplane, and contributes to the directional stability *and control* of the aeroplane, is considered to be a separate fin. (Thus, where surfaces extend both above and below a tailplane at the same spanwise station, they are counted as two fins if both upper and lower parts have rudders; if only one part has a rudder, it alone is regarded as a fin.)

(ii) All fins have the same moment arm (or an average value is taken).

(iii) Each fin, defined as in (i), has a height, h_{F_n}, and area, S_{F_n}. For body-mounted vertical fins h_{F_n}, and S_{F_n}, are as in Sketch 1.1. For tailplane-mounted vertical fins the root chord is defined relative to the upper or lower surface of the tailplane, as appropriate.

(iv) h_{F_n}, and S_{F_n} for inclined fins are taken as projected values in aeroplane plane of symmetry.

(v) For an imposed yawing moment, N_{asym}, due to asymmetry, the sideforce, Y_{F_n}, generated by each fin (cf. Equation (A1.1) is given by

$$Y_{F_n} = \left(\frac{S_{F_n}}{\Sigma S_{F_n}}\right)\frac{N_{asym}}{x_F} \tag{A2.5}$$

and

$$C_{Y_{F,n}} = \left(\frac{S_{F_n}}{\Sigma S_{F_n}}\right)\frac{N_{asym}}{qS_{F_n}x_F}. \tag{A2.6}$$

Following the sequence of equations in Section A2, the fin-induced contribution of each fin to aeroplane drag coefficient, based on wing reference area, is (cf. Equation (A2.4))

$$[(\Delta C_D)_{F,ind}]_n = \frac{K_F}{2\pi}\left[\left(\frac{S_{F_n}}{\Sigma S_{F_n}}\right)\frac{N_{asym}}{qx_F}\right]^2\frac{1}{Sh_{F_n}^2} \tag{A2.7}$$

so, for n fins,

$$(\Delta C_D)_{F,ind} = \frac{K_F}{2\pi}\left[\frac{N_{asym}}{qx_F}\right]^2\frac{1}{S}\frac{\Sigma\left(\frac{S_{F_n}}{h_{F_n}}\right)^2}{(\Sigma S_{F_n})^2}. \tag{A2.8}$$

Comparison of Equations (A2.4) and (A2.8) shows they are equivalent if,

$$\frac{1}{h_F^2} = \frac{\Sigma\left(\frac{S_{F_n}}{h_{F_n}}\right)^2}{(\Sigma S_{F_n})^2}. \tag{A2.9}$$

Equation (A2.9) defines the height, h_F of the equivalent single fin for a multiple-fin configuration. It was used successfully in incorporating in Figure 2 data for three aeroplanes.

APPENDIX B EXAMPLE OF WIND-TUNNEL DATA USED TO PREDICT DRAG DUE TO ASYMMETRY

Sketch B4.2 shows the results of wind-tunnel tests giving the variation of ΔC_D with sideslip, angle, β, and rudder angle, ζ, for a turbo-fan engined transport aeroplane with twin, wing-mounted engines in a take-off climb configuration (the same aeroplane is considered in the Example in Section 8). Determine values of ΔC_D in this configuration for flight with one engine inoperative, in ISA sea-level conditions (ρ = 0.002 376 9 slug/ft^3) for,

(i) W = 175 000 lbf, V = 143 kn, 241.4 ft/s, M = 0.2162, q = 69.2465 lbf/ft^2

(ii) W = 125 000 lbf, V = 121 kn, 204.2 ft/s, M = 0.1829, q = 49.578 86 lbf/ft^2 .

B1. AEROPLANE DATA AVAILABLE

B1.1 Geometric Data

S = 1400 ft^2 , b = 110 ft, l_p = 19 ft, x_F = 60 ft, S_F = 250 ft^2, h_F = 20 ft.

B1.2 Aerodynamic Data

In addition to the drag data given in Sketch B4.2, the following derivative values are given

$Y_v = -1.0$, $N_v = 0.2$, $Y_\zeta = 0.3$ per radian, $N_\zeta = -0.14$ per radian.

Ailerons and spoilers are assumed to make no significant contribution to forces or moments.

B1.3 Powerplant Data

For the given atmospheric conditions the net thrust, F_N, of the operating engine is as in Sketch B4.1. The drag due to the inoperative engine is given by the incremental value, D/q = 4.66 ft^2 (sum of windmilling- and spillage-drag contributions).

B2. CALCULATION OF MOMENT DUE TO ASYMMETRIC THRUST

The starboard engine is assumed inoperative (positive N_{asym}) and N_{asym} is expressed as

$$N_{asym} \approx [F_N + \text{drag of inoperative engine}]\, l_p .$$

For case (i), at M = 0.2162, Sketch B4.1 gives F_N = 20 950 lbf.

Since for this case, q = 69.2465 lbf/ft^2 ,

$$\begin{aligned} N_{asym} &= [20\,950 + (4.66 \times 69.2465)]\, 19 \\ &= [20\,950 + 323]\, 19 \\ &= 404\,181 \text{ lbf ft.} \end{aligned}$$

For case (ii), at $M = 0.1829$, Sketch B4.1 gives $F_N = 21\ 420$ lbf.

Since for this case, $q = 49.5789$ lbf/ft^2 ,

$$\begin{aligned} N_{asym} &= [21\ 420 + (4.66 \times 49.5789)]\ 19 \\ &= [21\ 420 + 231]\ 19 \\ &= 411\ 370 \text{ lbf ft.} \end{aligned}$$

B3. CALCULATION OF EQUILIBRIUM FLIGHT CONDITIONS

Where there are no effects due to aileron or spoiler deflections, the general expressions of Equations (4.12) and (4.14) in Section 4.1 may be solved as in Section 4.2.3 to give Equations (4.31) and (4.32) for rudder angle to trim and sideslip angle respectively.

B3.1 Case (i), $W = 175\ 000$ lbf, $V = 143$ kn

Substituting values into Equations (4.31) and (4.32) gives

$$\zeta = \frac{-1}{-0.14}\left[\frac{404\ 181}{69.2465 \times 1400 \times 110} + 0.2 \sin\beta\right]$$

$$= 0.270\ 726 + 1.428\ 57 \sin\beta\ ,$$

$$\sin\beta = \frac{1}{69.2465 \times 1400} \frac{\left[\frac{0.3 \times 404\ 181}{(-0.14) \times 110} - 175\ 000 \sin\Phi \cos\Theta\right]}{\left[-1 - \left(\frac{0.3}{-0.14} \times 0.2\right)\right]}$$

$$= 0.142\ 131 + 3.1590 \sin\Phi \cos\Theta\ .$$

For $\Theta = 12$ deg, $\sin\beta = 0.142\ 131 + 3.089\ 97 \sin\Phi$.

Values of β and ζ are calculated in the following table for a range of values of Φ for $\Theta = 12$ deg. This value of Θ is typical for take-off climb with one engine failed, but the effect of putting $\Theta = 0$ and $\Theta = 18$ deg is also demonstrated numerically in the table. The calculated values of β and ζ for $\Theta = 12$ deg are plotted in Sketch B4.2, the corresponding values of ΔC_D are read off and are presented in the last column of the table.

Θ deg	Φ deg	$\sin\beta$	β deg	ζ rad	ζ deg	ΔC_D
12	0	0.142131	8.1712	0.47377	27.145	0.0114
	–1	0.088203	5.0603	0.39673	22.731	0.00935
	–2	0.034292	1.9652	0.31971	18.318	0.0069
	–3	–0.019586	–1.1223	0.24275	13.908	0.0058
	–4	–0.073415	–4.2101	0.16585	9.502	0.0068
	–5	–0.127178	–7.3065	0.08904	5.102	0.0104
0	0	0.142131	8.1712	0.47377	27.145	0.0114
	–2	0.031883	1.8271	0.31627	18.121	0.0069
	–5	–0.13319	–7.6542	0.08045	4.609	0.0109
18	0	0.142131	8.1712	0.47377	27.145	0.00114
	–2	0.37279	2.1364	0.32398	18.563	0.00685
	–5	–0.11972	–6.8759	0.09970	5.712	0.01055

B3.2 Case (ii), $W = 125\,000$ lbf, $V = 121$ kn

Substituting values into Equations (4.31) and (4.32) gives

$$\zeta = \frac{-1}{-0.14}\left[\frac{411\,370}{49.5789 \times 1400 \times 110} + 0.2\sin\beta\right]$$

$$= (0.384\,846 + 1.428\,57\sin\beta),$$

$$\sin\beta = \frac{1}{49.5789 \times 1400}\,\frac{\left[\frac{0.3 \times 411\,370}{(-0.14) \times 110} - 125\,000\sin\Phi\cos\Theta\right]}{\left[-1 - \left(\frac{0.3}{(-0.14)} \times 0.2\right)\right]}$$

$$= 0.202\,044 + 3.151\,54\sin\Phi\cos\Theta.$$

For $\Theta = 12$ deg, $\sin\beta = 0.202\,044 + 3.082\,68\sin\Phi$.

Values of β and ζ are calculated in the following table for a range of values of Φ for $\Theta = 12$ deg. See Section B3.1 regarding likely effects of changes in Θ. The calculated values of β and ζ are plotted in Sketch B4.2, the corresponding values of ΔC_D are read off and are presented in the last column of the table.

Θ deg	Φ deg	$\sin\beta$	β deg	ζ rad	ζ deg	ΔC_D
12	0	0.20204	11.6565	0.67348	38.588	–
	–1	0.14824	8.5252	0.59662	34.184	–
	–2	0.09446	5.4203	0.51979	29.782	0.0135
	–3	0.04071	2.3331	0.44300	25.382	0.013
	–4	–0.01299	–0.7444	0.36620	20.987	0.01225
	–5	–0.06663	–3.8204	0.28966	16.596	0.01305
	–6	–0.12018	–6.9027	0.21316	12.213	0.0157

B4. ESTIMATION OF DRAG COEFFICIENT INCREMENTS DUE TO THRUST ASYMMETRY

Values of β and ζ calculated in Sections B3.1 and B3.2 for steady straight trimmed flight at $\Theta = 12$ deg are plotted in Sketch B4.2 and corresponding values of ΔC_D read off for each flight condition, see tables in those Sections. (Note that values of β and ζ for $\Theta = 0$ and 18 deg calculated in the table in Section B3.1, would plot on virtually the same line as the data for $\Theta = 12$ deg in case (i).)

While values of ΔC_D vary with flight condition, one effect of the minima exhibited by the curves is that for considerable ranges of values of β, ζ, Φ, the value of ΔC_D might be taken as constant,

i.e. for case (i), $\Delta C_D \approx 0.006$ and

for case (ii), $\Delta C_D \approx 0.013$.

A brief comparison of the results obtained here and in Section 8 is given in the latter.

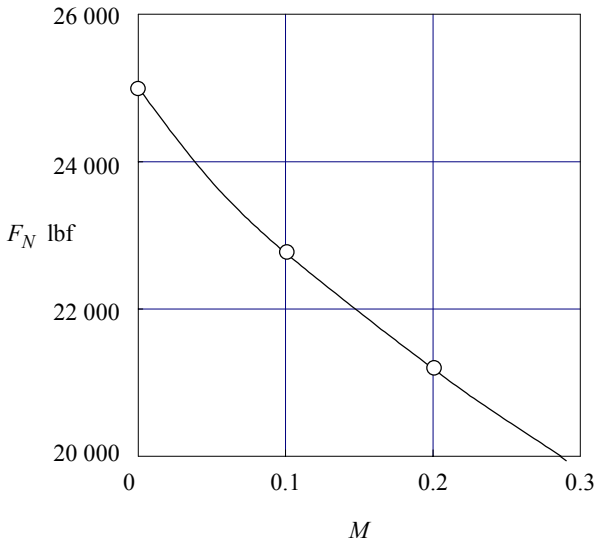

Sketch B4.1 Net thrust of operating engine

Sketch B4.2 Drag coefficient increments due to rudder and sideslip angles for equilibrium flight conditions calculated in Sections B3.1 and B3.2

THE PREPARATION OF THIS DATA ITEM

The work on this particular Data Item was monitored and guided by the Performance Committee, which first met in 1946 and now has the following membership:

Chairman
Mr W.L. Horsley – Civil Aviation Authority, Airworthiness Division

Vice Chairman
Mr A.N. Page – British Aerospace (Commercial Aircraft) Ltd, Hatfield

Members
Mr K.J. Balkwill – British Aerospace (Military Aircraft) Ltd, Brough
Mr T.B.A. Boughton – Independent
Mr E.N. Brailsford – Independent
Mr T. Duxbury – British Aerospace (Military Aircraft) Ltd, Warton
Mr P.D. Feig* – General Electric Company, Cincinnati, Ohio, USA
Mr N.J. Herniman – Airbus Industrie
Mr R.G. Humpston – Rolls-Royce Ltd, Derby Engine Division
Mr L.R. Jenkinson – Loughborough University of Technology
Mr T.S.R. Jordan – Independent
Mr J.R.D. Kenward – Independent
Mr R. Kita* – Grumman Aircraft Systems, Bethpage, NY, USA
Mr W.T. Lewerenz* – McDonnell Douglas, Long Beach, Calif., USA
Mr E.J. Norris – Aeroplane and Armament Experimental Establishment
Mr. P. Robinson – British Aerospace Headquarters, Weybridge
Mr D.A. Schelp* – Boeing Commercial Airplane Company
Mr G.E. Smith – Ministry of Defence, Procurement Executive
Prof. E. Torenbeek* – Delft University of Technology
Mr J.D. Wiles – British Airways.

* Corresponding Member

The technical work involved in the assessment of the available information and the construction and subsequent development of the Data Item was undertaken by

Mr D.J. Mitchell – Group Head.

Particular assistance in the form of a preliminary study of the subject matter was received from Mr P. Zondervan, a student with Delft University of Technology. The person with overall responsibility for the work in this subject area is Mr D.J. Mitchell.